

U. S. AIR FORCE

PROJECT RAND

RESEARCH MEMORANDUM

CLOSE-IN-H-BOMB EFFECTS

H. L. Brode

RM-1583-1

ASTIA DOCUMENT NUMBER AD 144275

November 11, 1955

Revised February 3, 1956

Assigned to _____

This research is sponsored by the United States Air Force under contract No. AF 49(638)-700 monitored by the Directorate of Development Planning, Deputy Chief of Staff, Development, Hq USAF.

This is a working paper. It may be expanded, modified, or withdrawn at any time. The views, conclusions, and recommendations expressed herein do not necessarily reflect the official views or policies of the United States Air Force.

The **RAND** *Corporation*

1700 MAIN ST. • SANTA MONICA • CALIFORNIA

CLOSE-IN H-BOMB EFFECTS

I. INTRODUCTION

Recent concern with the chances of survival for relatively invulnerable structures and with the design of protective structures has led us to consider the damage due to blast, thermal, and nuclear radiations from an H-bomb in regions of greater intensity than have been previously considered important to military effects. Some aspects of the nuclear explosion remain unchanged in quality and merely increase in intensity as one moves closer to the bomb burst. Other phenomena, however, change their character sufficiently to warrant a special re-evaluation.

For example the nature of nuclear radiations may be expected to be somewhat different. The mean energy, and so the penetrating power and biological effectiveness of neutrons and gamma rays will be increased, and at the same time the rate and direction of dose delivery will be altered. Also in this close-in region the type of weapon and the details of its nucleonics will be of even greater concern. In addition we may expect large hydrodynamic effects on these doses.

In these close-in regions one may expect quite different thermal radiations. Not only will the frequency and time distributions of radiative flux be quite different than that at large distances but here any point will also be engulfed in the superheated air of the fireball itself.

Here, too, the nature of the blast wave is changed. Such quantities as positive phase duration or total impulses cannot enjoy the same significance that they do at larger distances. Aside from complications due to interaction with radiative processes and the break-down of the ideal gas assumption for air, we encounter radically different time and space histories of the blast parameters. Pressure pulses are exceedingly rapid in both rise and decay and have much greater dynamic effects. Here also we encounter hypersonic flow problems. On the other hand non-ideal surface effects may be reduced. (Strong shocks tend to be less influenced by local irregularities.) It is conceivable that precursor phenomena may not have as large an influence on the blast waves. Although the interactions between the various weapon effects is strongest in this close-in region, and although the details of bomb physics and bomb design are of greater significance here, the general nature of the free-field blast wave may still be adequately well described by a simple hydrodynamic model (using initial conditions compatible with the earlier radiative effects). The next section contains the results of detailed computations on such a model.

II. BLAST

At present measurements in the region of high levels of pressure are scanty and restricted to indirect or simple peak value measures such as fireball growth photography, time-of-arrival data and ball-crusher or beer-can type gauges. The very nature of this region has heretofore precluded extensive measurements and consequently no details of dynamic effects and time histories of pressure pulses are available from tests. For this reason, the curves offered in this section cannot be claimed to be verified in detail.

However, whenever comparisons with test results are available their satisfactory agreement with these theoretical solutions speaks well for the reliability of both the theory and the data.

However, the important question as to how well the results of these calculations predict blast loading from a nuclear bomb explosion cannot be answered with any certainty at present. The following qualitative evaluation may be useful, however:

- 1.) In general a strong shock is less influenced by thermal gradients or variable conditions in the medium through which it propagates. For this reason one could expect sharper rises and cleaner shocks in this close-in region.
- 2.) Since strong shocks are characterized by very sharp rise and decay in both time and space the influence of multiple shocks and disturbances in the after-flow, due to local interferences and reflections, is minimized in problems of structural response.
- 3.) On the other hand, in the close-in regions the blast has not always developed far enough from its earliest stages to have washed out the influences of multiple bomb shock and initial radiation transport effects. Neglect of this is in general not serious, but in very special instances may mean overlooking a sudden increase in the main shock strength by as much as 20 per cent.
- 4.) Surface phenomena such as the thermal precursor should be of minor influence for any height of burst at these high levels of blast, since here the blast arrives before the bulk of the thermal radiation is received.

5.) The hypersonic flow at shock and particle speeds of many Mach may also lead to peculiar loading problems, locally.

The curves presented are the result of numerical integration of the partial differential equations of gas motion. The calculational detail includes the use of a careful fit to the equation of state for air and an entirely general treatment of the gas dynamics (no restricting similarity assumptions, for instance).

In particular the curves presented here stem from a calculation whose initial conditions characterize a point source. Calculations also have been carried out which start from an isothermal sphere approximating the effect of radiation diffusion on the early stages of a nuclear bomb explosion. The essential character of the subsequent blast wave in these latter calculations matches that of the point-source calculation. In detail, however, the isothermal-sphere calculations are encumbered by the presence of multiple minor shocks and rarefactions. For this reason it was felt that the point-source case was more appropriate from the standpoint of simplicity and generality and for ease in scaling and analytical fitting.

The results of these calculations which include the equation of state of air do not differ from the previous ideal-gas calculations in the lower pressure regions ($\Delta P_g < 3$ atmos) but they show some marked differences in dynamic pressures, densities and temperatures in the higher pressure regions.

The general methods employed in these calculations are similar to those described in an article by this author which appeared in the Journal of Applied Physics⁽¹⁾ (June 1955) and which covers the ideal-gas computations.

All the curves are scaled to a two megaton free-air burst, with the intent that they should be used as representative of a one megaton surface burst.

¹ H. L. Brode, J. of Appl. Phys. 26 766-775 (June 1955).

They also represent burst in a homogeneous sea-level atmosphere with standard ambient pressure $P_0 = 14.7$ psi, density $\rho_0 = .00129$ gm/cc, and temperature $T_0 = 273.2$ °Kelvin.

Any other yield or ambient conditions are achieved by multiplying all distances by $(W/\pi)^{1/3}$ and all times by $(W/\pi)^{1/3} \tau^{-1/2}$ where W is the yield in megatons, π is the ratio of ambient pressure (P_a) to standard pressure (P_0), and τ is the ratio of ambient temperature (T_a) to standard temperature (T_0). Under this scaling the various pressure ratios will be the same, but pressures must be multiplied by π , velocities (Mach numbers) by $\tau^{1/2}$ and temperatures by τ^1 .

Figure 1. is a plot of peak overpressure in atmospheres (14.7 psi) versus range in kilofeet.

Figure 2. is a similar plot of the peak dynamic pressure ($1/2 \rho u^2$) in atmospheres versus range in kilofeet. It should be noted that the usual Hugoniot relation for an ideal gas of $\gamma = 1.4$, viz. $Q_s = \frac{5}{2} \frac{\Delta P_s^2}{7P_0 + \Delta P_s}$ is valid only for small pressures ($\Delta P_s < 3$ atmos), and that for higher pressures the peak dynamic pressures are greater than this (characteristic of a smaller γ).

Figure 3. is a plot of particle velocity (u_s) and shock velocity (U_s) in units of ambient sonic velocity, i.e., a plot of particle and shock Mach numbers. Also plotted is the shock density (ρ_s) in units of ambient density (ρ_0) versus range in kilofeet.

Figures 4 - 21 are plots of overpressure (ΔP) in atmos, dynamic pressure (Q) in atmos, particle Mach number (U), density ratio (ρ), and temperature ratio

($\theta = T/T_0$) versus time in seconds at various distances from the burst.

Figure 22. is a plot of various parameters versus the shock overpressure (ΔP_s) in atmos. Definition of these parameters is as follows:

Q_s = shock dynamic pressure ($1/2 \rho_s U_s^2$)

t_s = time of arrival of shock (sec)

D_P^+ = duration of pressure positive phase (sec)

D_Q^+ = duration of dynamic-pressure positive phase (sec)

Δ_P^s = duration of the right-triangular pulse having the same initial slope as the true pressure pulse (sec)

Δ_Q^s = duration of the right-triangular dynamic-pressure pulse having the same initial slope as the true dynamic pressure pulse (sec)

α = exponent coefficient for early part of pressure pulse fitted by the form $\Delta P = \Delta P_s e^{-\alpha t}$

β = exponent coefficient for early part of dynamic-pressure pulse fitted by the form $Q = Q_s e^{-\beta t}$

Figures 21 & 22 show some of the plotted parameters as a function of radius for various times in the course of the explosion.

Figure 1

Peak Overpressure vs Distance from a
1 MT Surface Burst

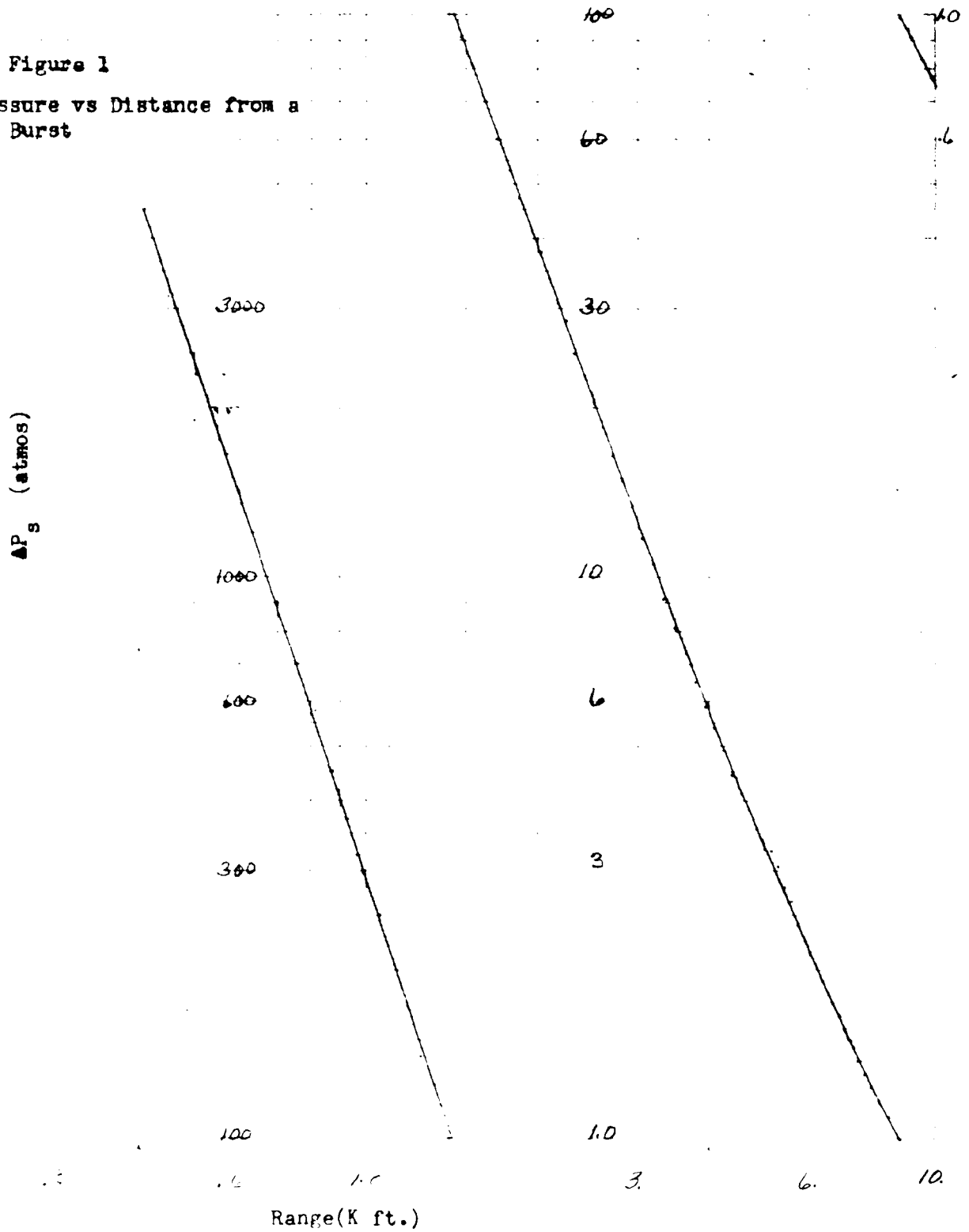
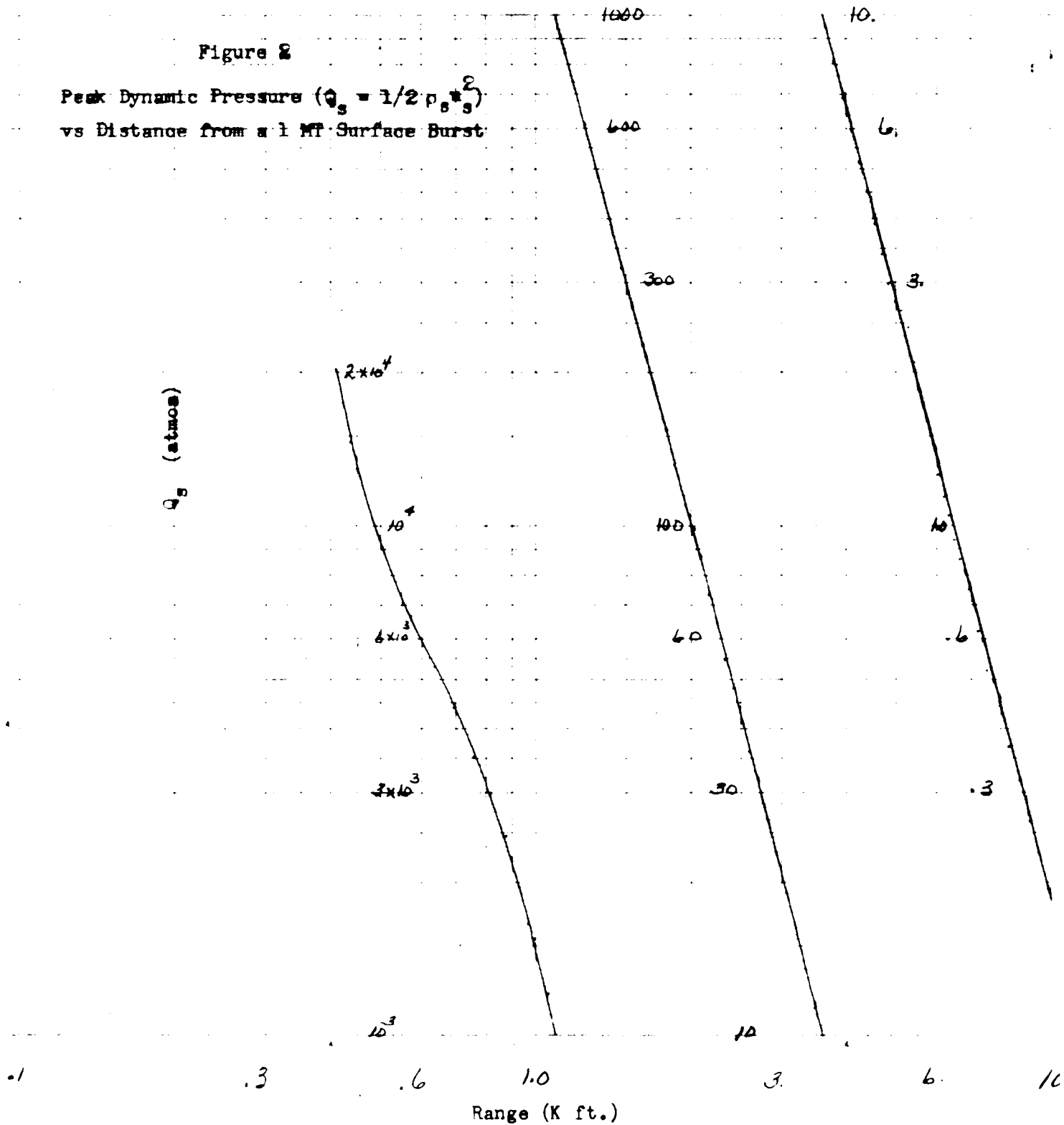


Figure 2

Peak Dynamic Pressure ($Q_s = 1/2 \rho_s v_s^2$)
vs Distance from a 1 MT Surface Burst



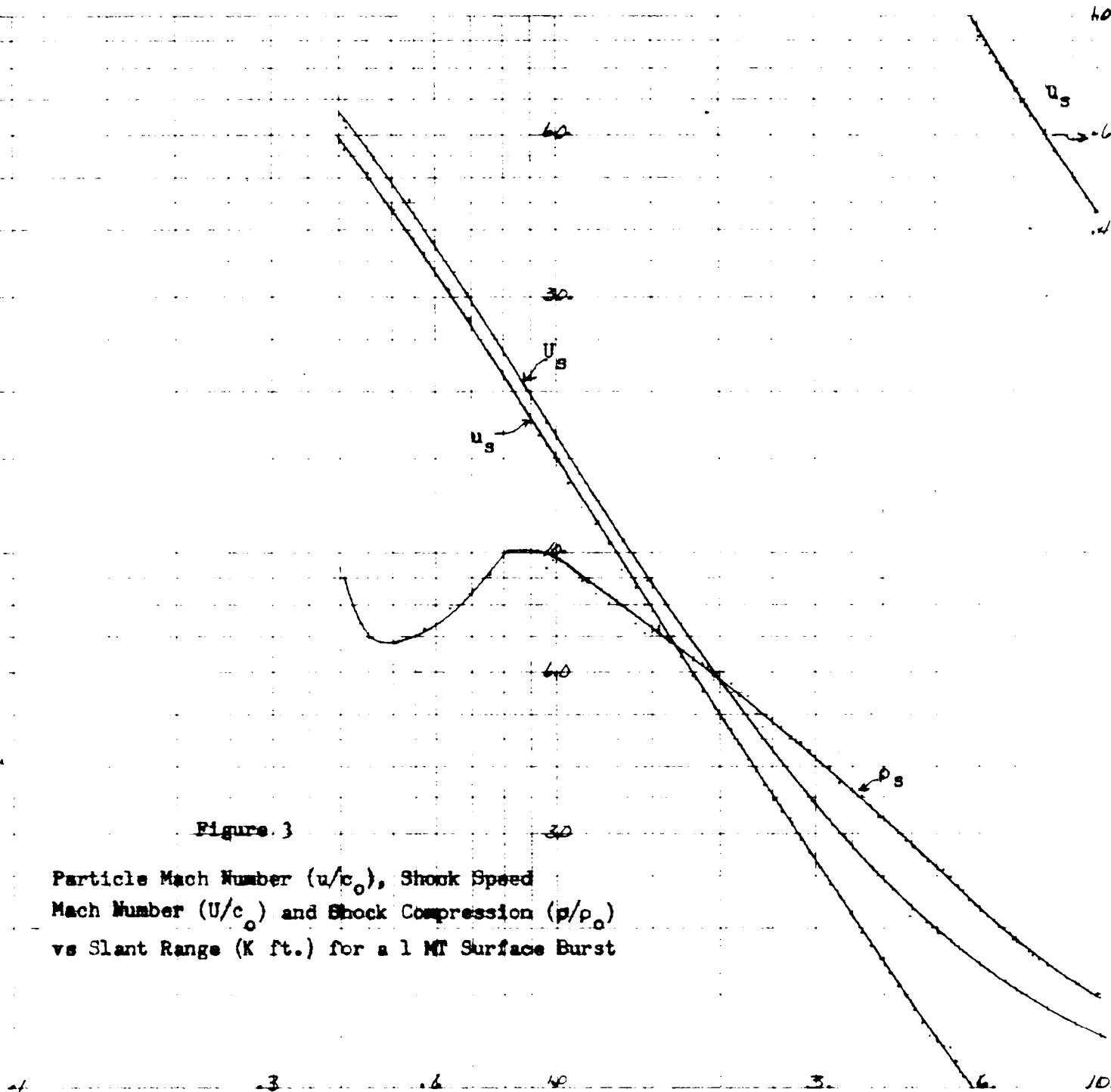


Figure 3

Particle Mach Number (u/c_0), Shock Speed
Mach Number (U/c_0) and Shock Compression (p/p_0)
vs Slant Range (K ft.) for a 1 MT Surface Burst

Range (K ft.)

Figure 4

Blast Parameters as Functions of Time
at 695 Feet from a 1 MT Surface Burst

$$\Delta P_s = 900 \text{ atmos.}$$

$$Q_s = 4.39 \times 10^3 \text{ atmos.}$$

$$t_s = .00807 \text{ sec.}$$

$$T_s = \theta_s T_0 = 1.37 \times 10^4 \text{ } ^\circ\text{K}$$

$$\rho_s = 8.40$$

$$v_s = u_s c_0 = 2.97 \times 10^4 \text{ feet/sec.}$$

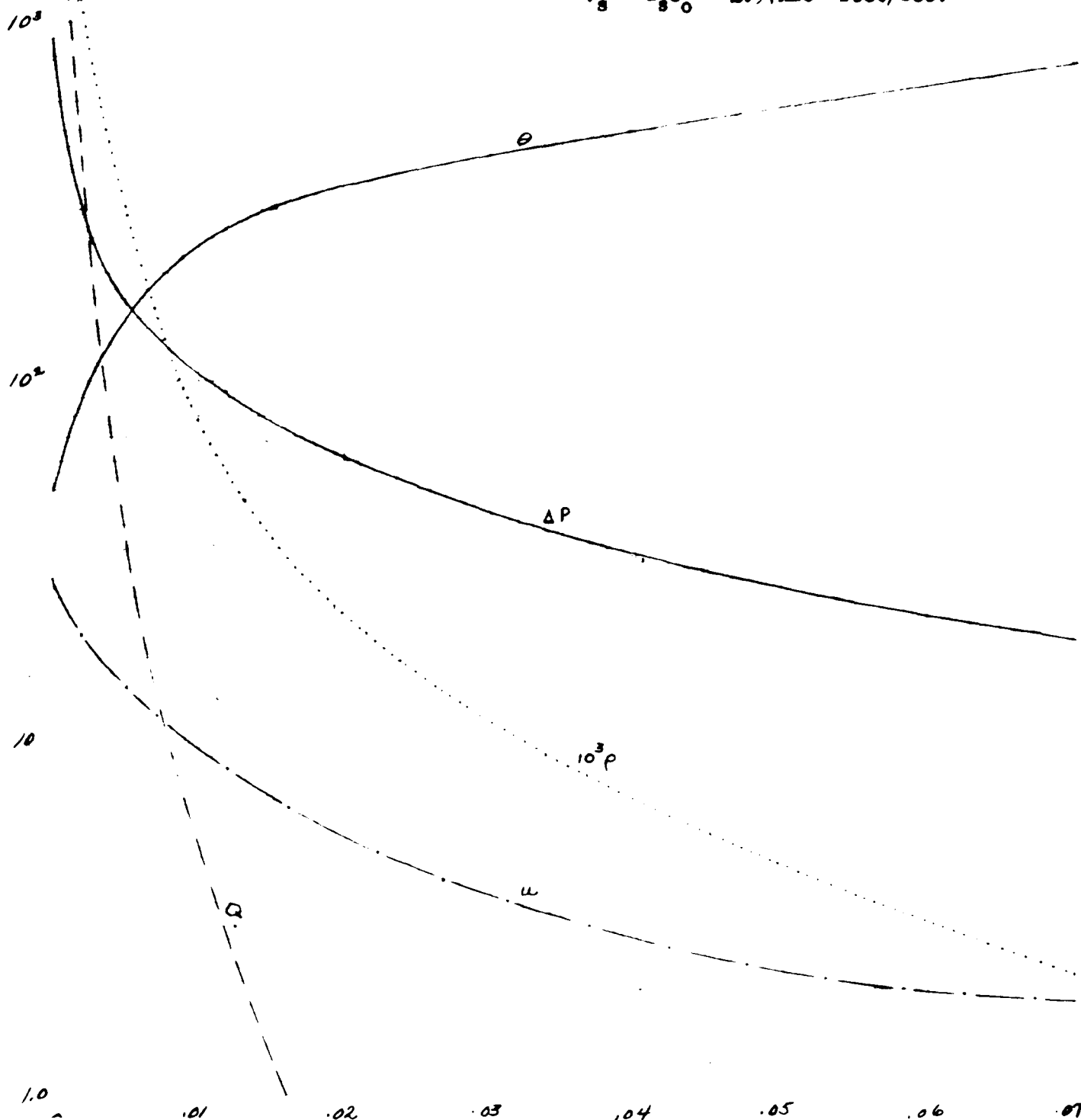


Figure 5

Blast Parameters as Functions of Time
at 755 feet from a 11MT Surface Burst

$$\Delta P_s = 699 \text{ atmos.}$$

$$Q_s = 3.51 \times 10^3 \text{ atmos.}$$

$$t_s = .00992 \text{ sec.}$$

$$T_s = \theta_s T_\theta = 1.09 \times 10^4 \text{ } ^\circ\text{K}$$

$$\rho_s = 9.11$$

$$v_s = u_s c_0 = 2.55 \times 10^4 \text{ feet/sec.}$$

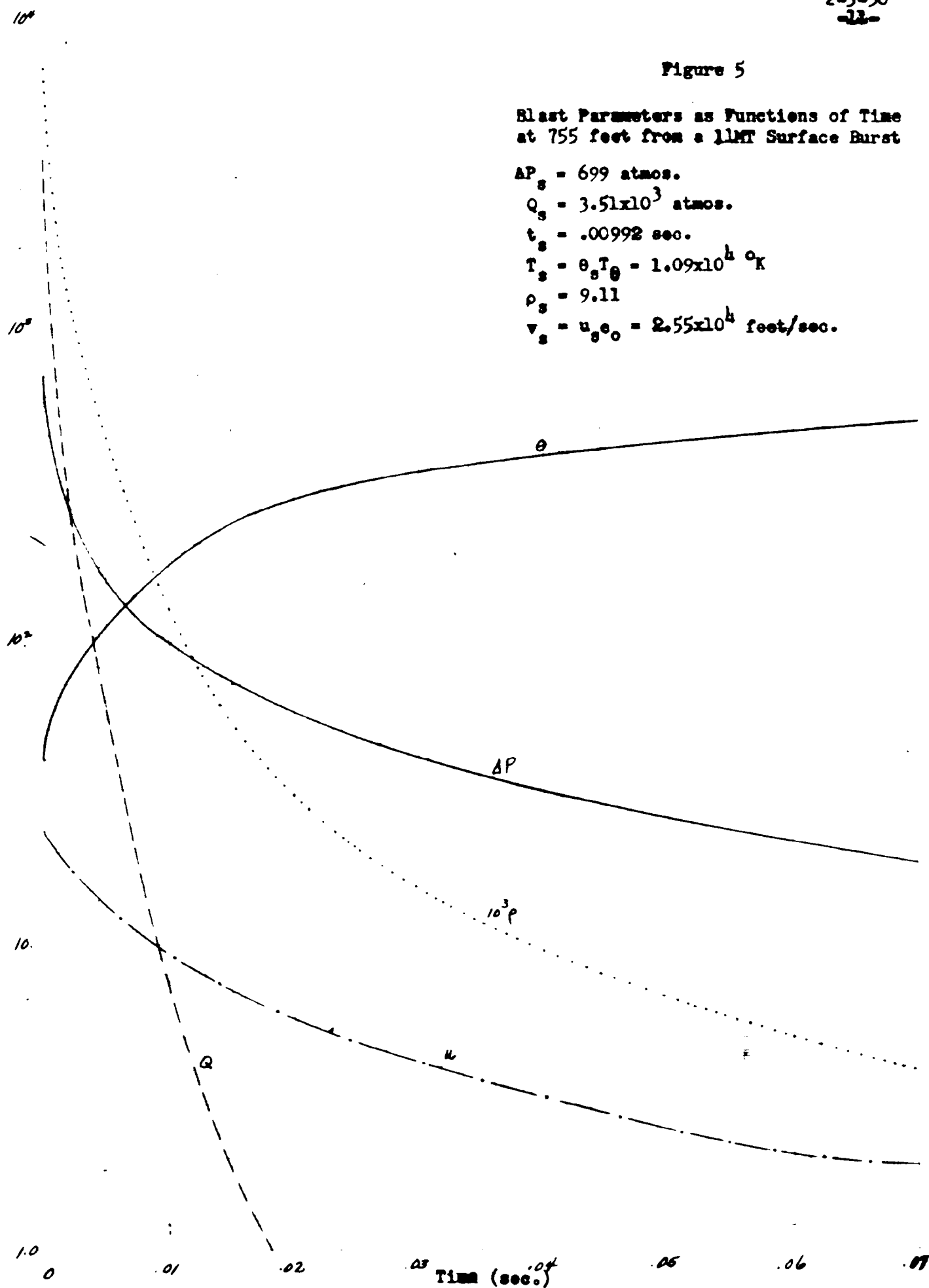


Figure 6

Blast Parameters as Functions of Time
at 874 feet from a 1 MT Surface Burst

$$\Delta P_s = 452 \text{ atmos.}$$

$$Q_s = 2.47 \times 10^3 \text{ atmos.}$$

$$t_s = .0144 \text{ sec.}$$

$$T_s = \theta_s T_0 = 7.79 \times 10^3 \text{ } ^\circ\text{K}$$

$$\rho_s = 10.1$$

$$v_s = u_s c_0 = 2.03 \times 10^4 \text{ feet/sec.}$$

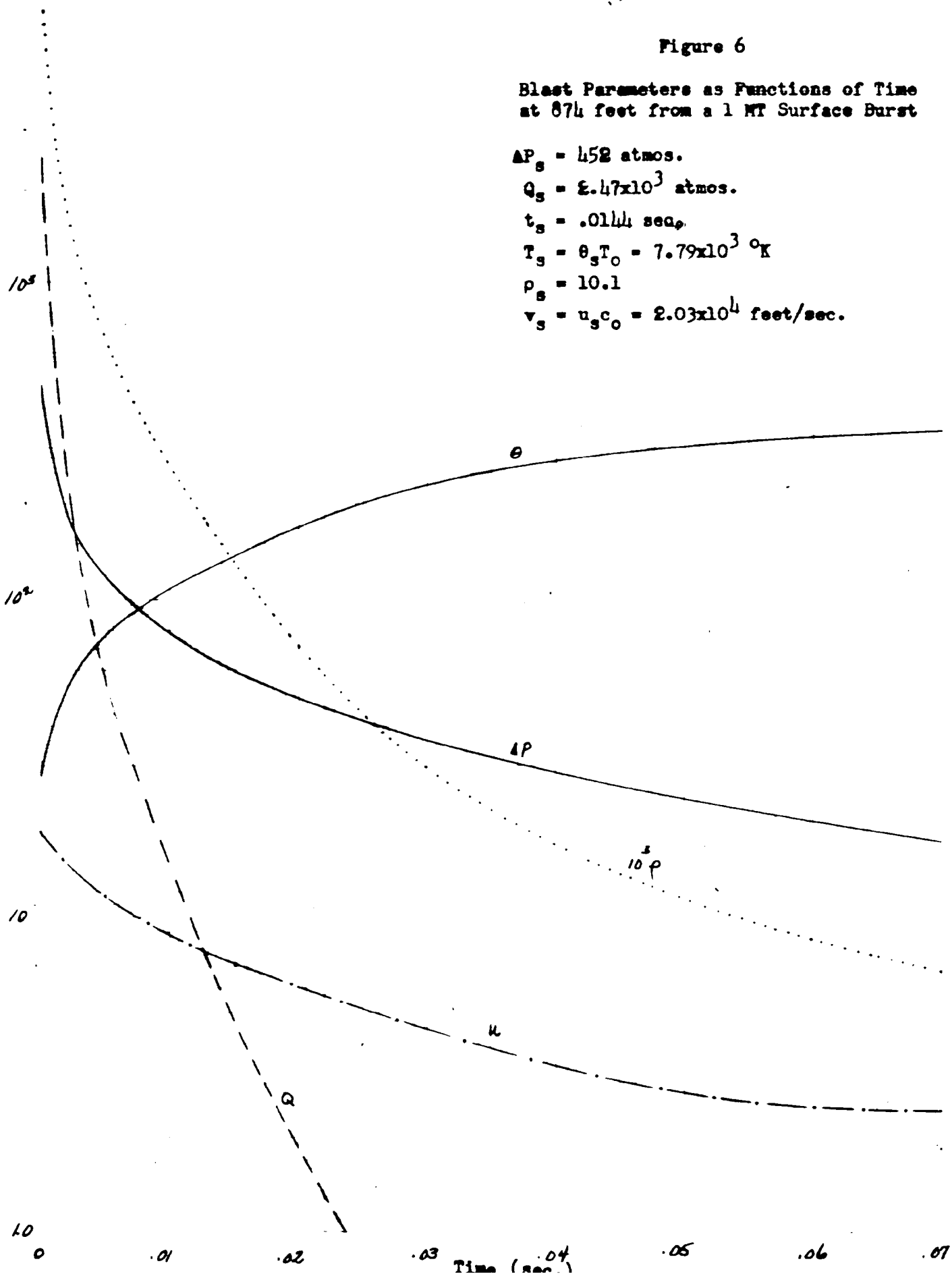


Figure 7

Blast Parameters as Functions of Time
at 994 feet from a 1 MT Surface Burst

$$\Delta P_s = 297 \text{ atmos.}$$

$$Q_s = 1.55 \times 10^3 \text{ atmos.}$$

$$t_s = .0200 \text{ sec.}$$

$$T_s = \theta_s T_0 = 6.19 \times 10^3 \text{ } ^\circ\text{K}$$

$$\rho_s = 9.67$$

$$v_s = u_s c_0 = 1.64 \times 10^4 \text{ feet/sec.}$$

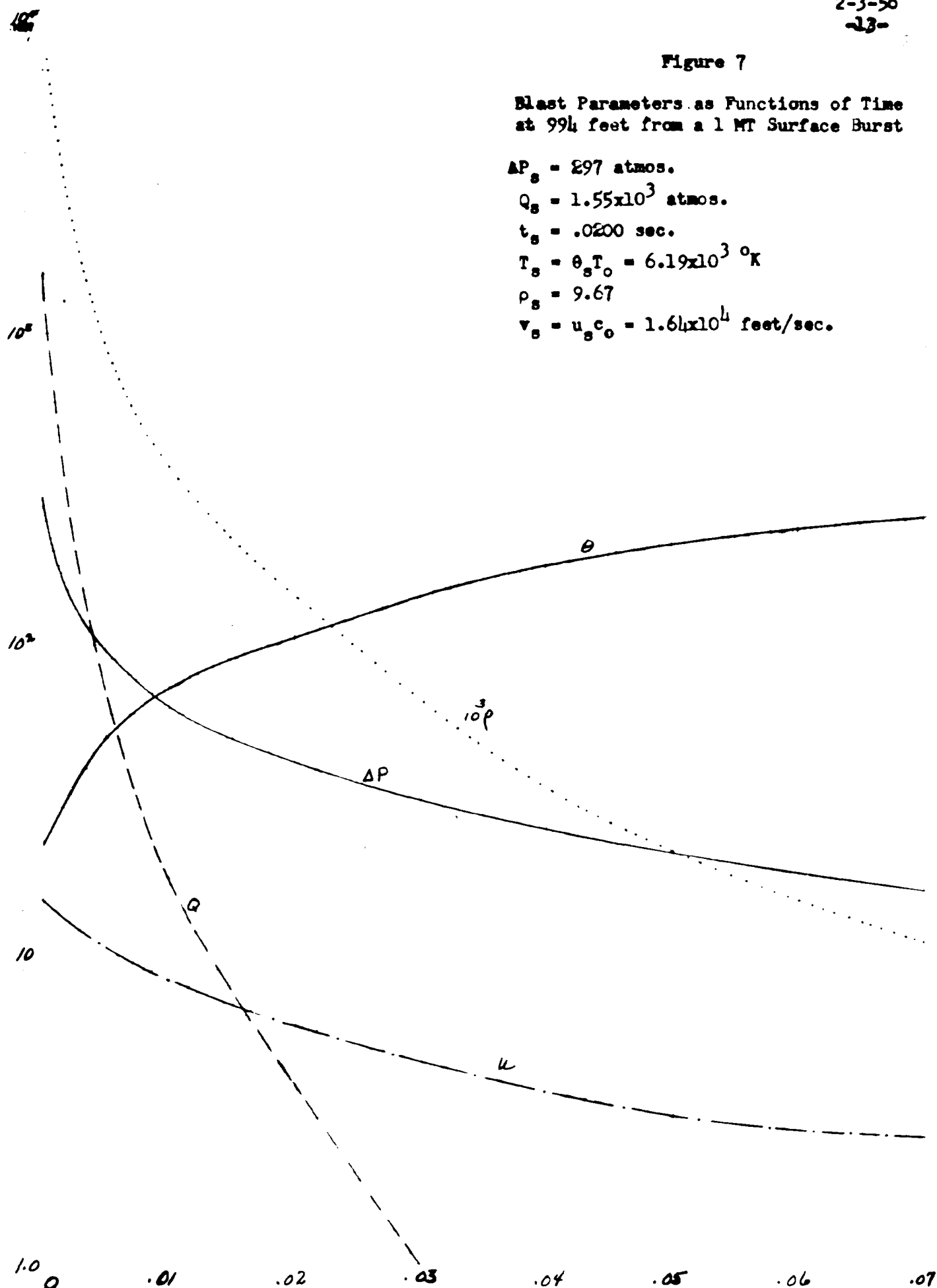


Figure 8

Blast Parameters as Functions of Time
at 1120 feet from a 1 MT Surface Burst

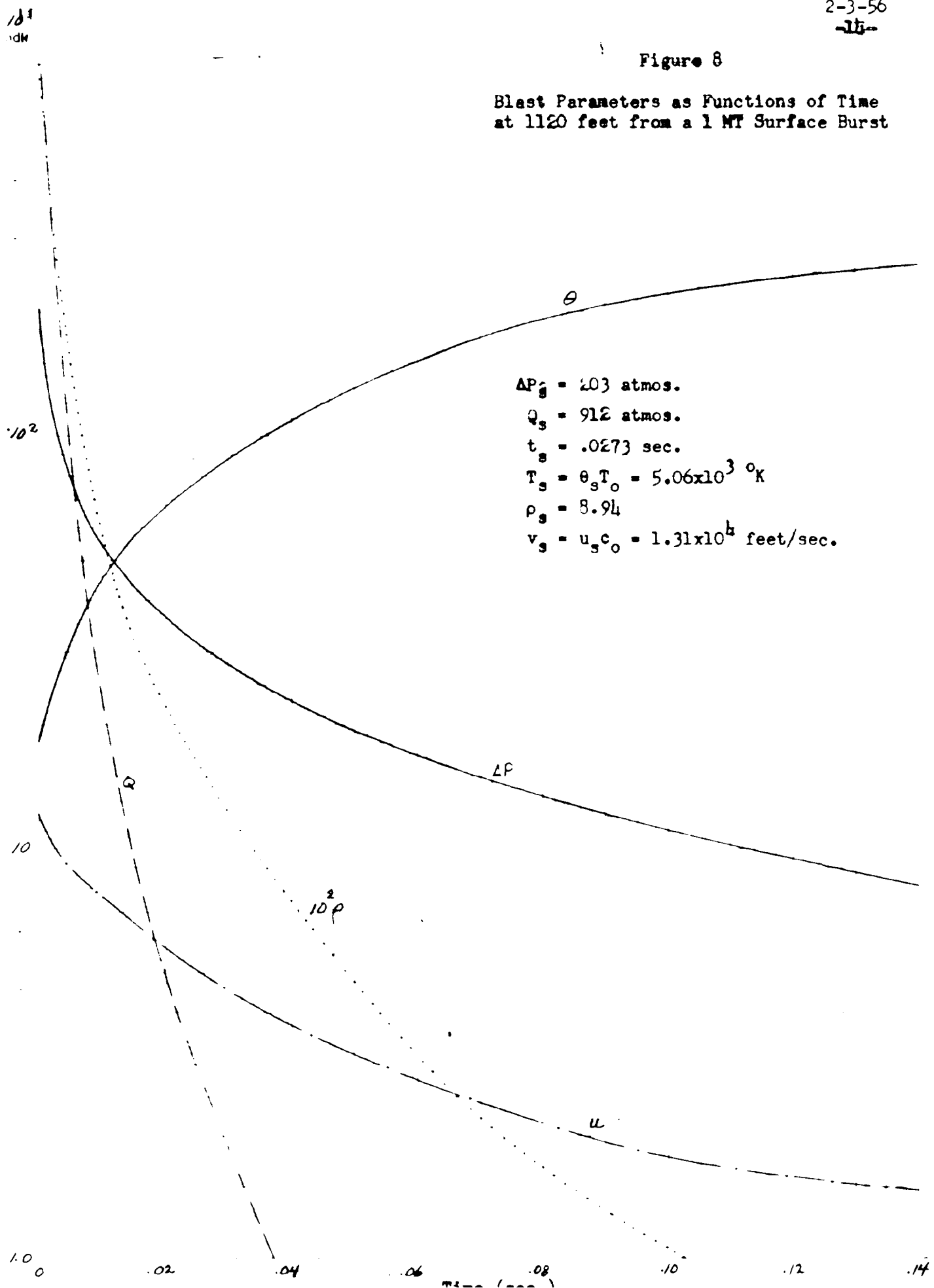


Figure 9

Blast Parameters as Functions of Time
at 1395 feet from a 1 MT Surface Burst

$$\Delta P_s = 99.9 \text{ atmos.}$$

$$Q_s = 385 \text{ atmos.}$$

$$t_s = .0479 \text{ sec.}$$

$$T_s = \theta_s T_o = 3.41 \times 10^3 \text{ } ^\circ\text{K}$$

$$\rho_s = 7.36$$

$$v_s = u_s c_o = 9.40 \times 10^3 \text{ feet/sec.}$$

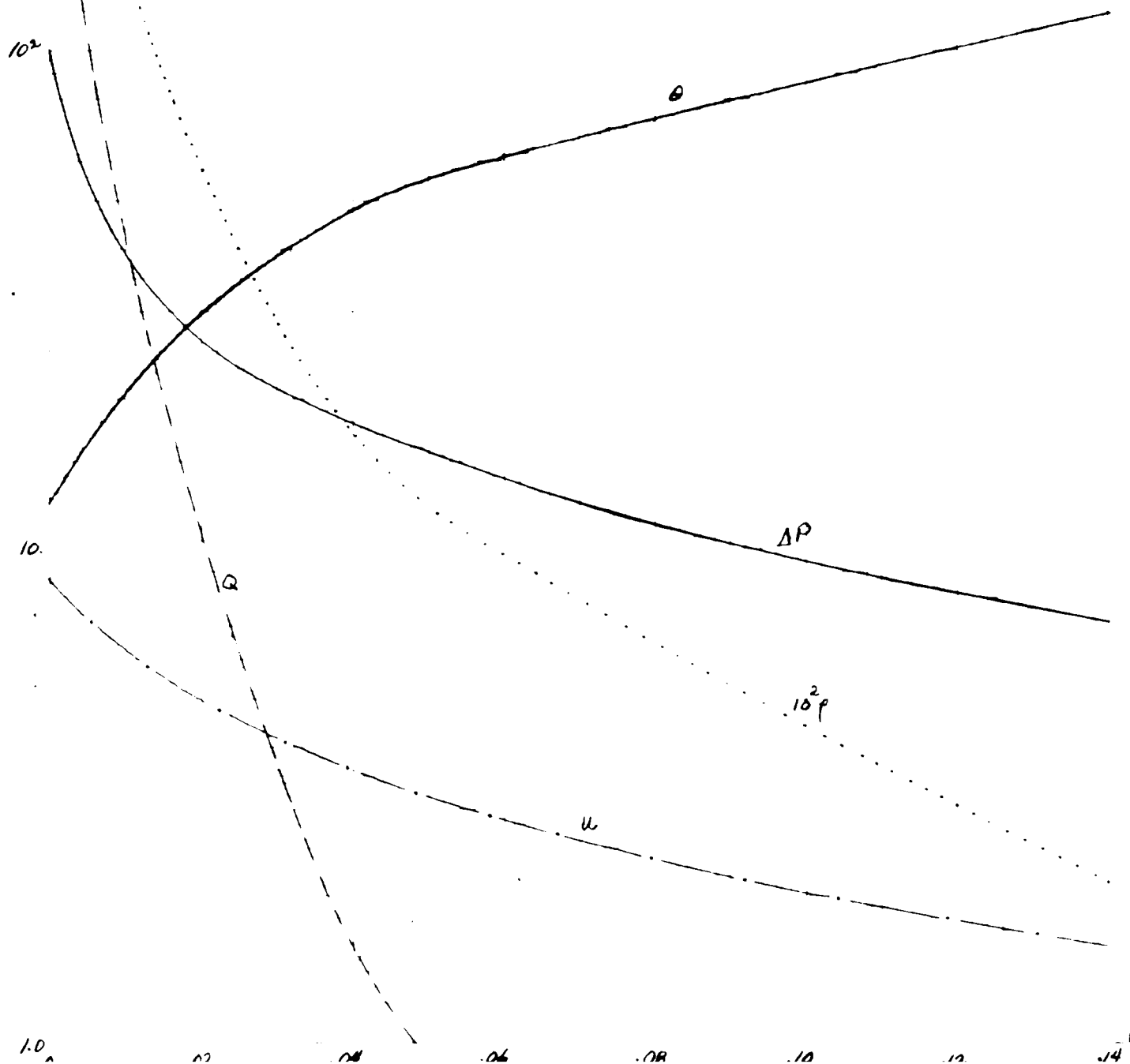


Figure 10

Blast Parameters as Functions of Time
at 1621 feet from a 1 MT Surface Burst

$$\Delta P_s = 69.9 \text{ atmos.}$$

$$Q_s = 227 \text{ atmos.}$$

$$t_s = .0699 \text{ sec.}$$

$$T_s = \theta_s T_0 = 2.66 \times 10^3 \text{ } ^\circ\text{K}$$

$$\rho_s = 6.86$$

$$v_s = u_s c_0 = 7.47 \times 10^3 \text{ feet/sec.}$$

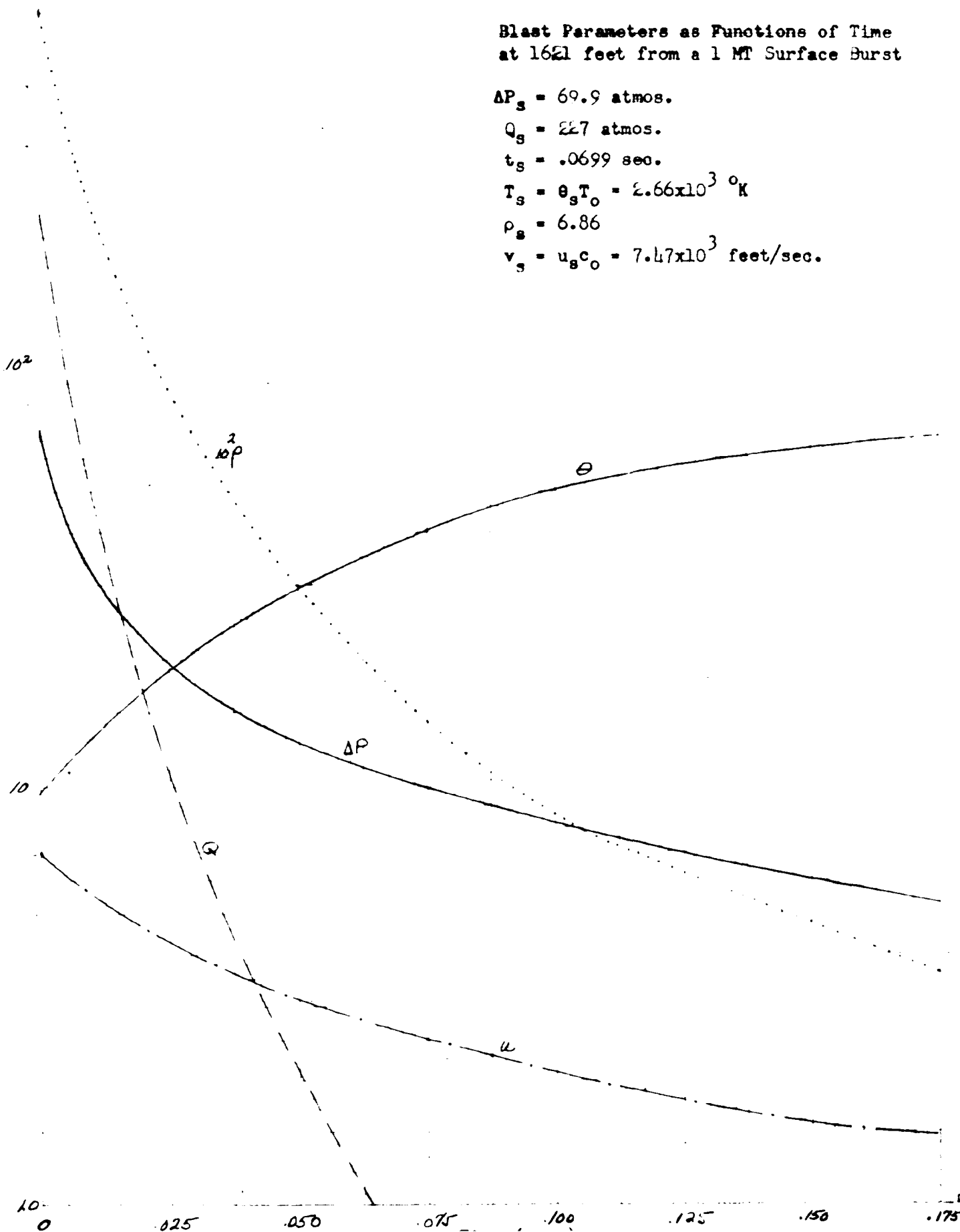
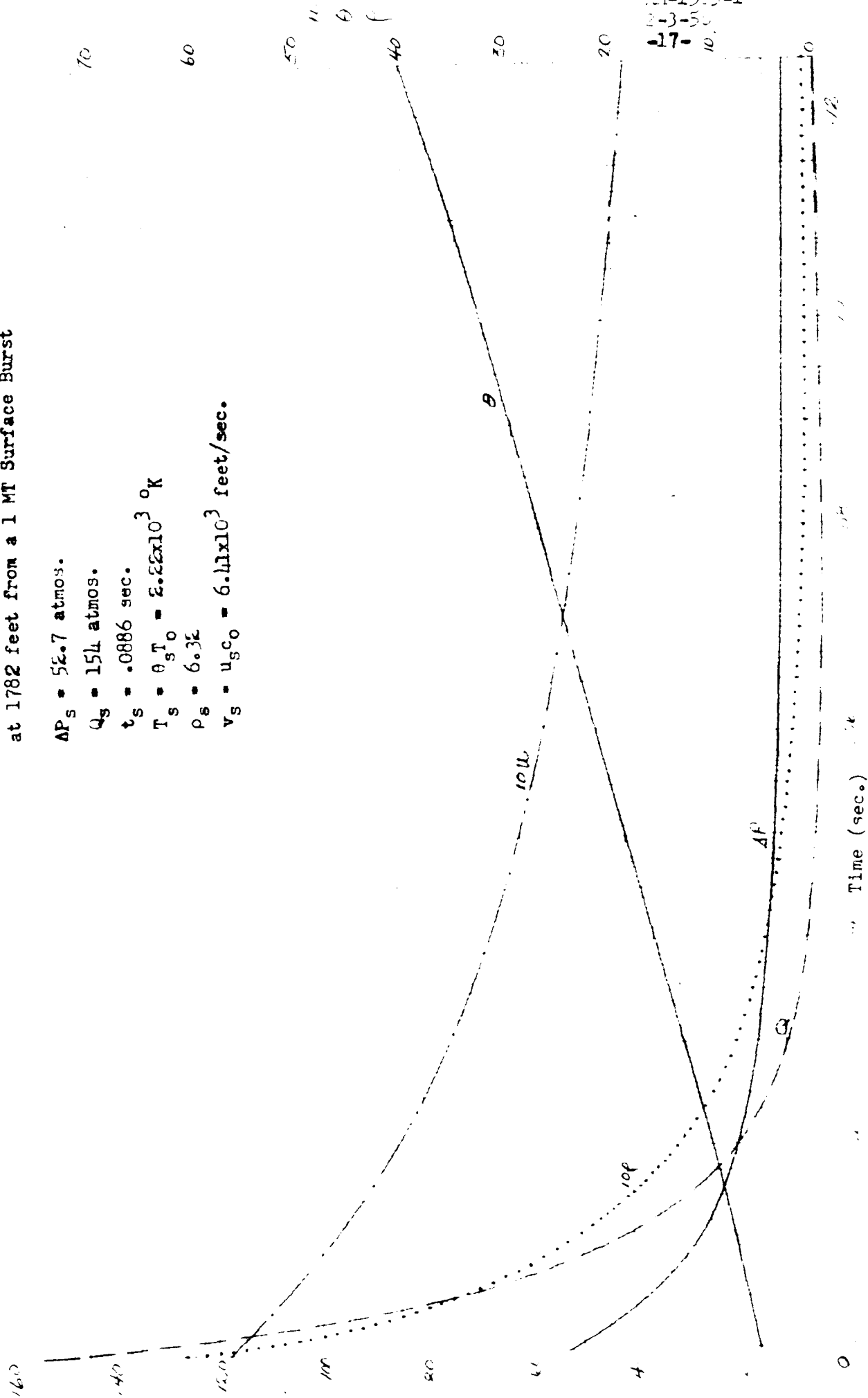


Figure 11

Blast Parameters as Functions of Time
at 1782 feet from a 1 MT Surface Burst

$\Delta P_s = 52.7$ atmos.
 $Q_s = 154$ atmos.
 $t_s = .0886$ sec.
 $T_s = \theta_s T_0 = 2.22 \times 10^3$ °K
 $\rho_s = 6.32$
 $v_s = u_{s0} = 6.41 \times 10^3$ feet/sec.



EM-1533-1
 2-3-50
 -17- 10

Figure 12

Blast Parameters as Functions of Time
at 2172 feet from a 1 MT Surface Burst

$$\Delta P_s = 30.6 \text{ atmos.}$$

$$Q_s = 72.8 \text{ atmos.}$$

$$t_s = .144 \text{ sec.}$$

$$T_s = \theta_s T_0 = 1.56 \times 10^3 \text{ } ^\circ\text{K}$$

$$\rho_s = 5.42$$

$$v_s = u_s c_0 = 4.76 \times 10^3 \text{ feet/sec.}$$

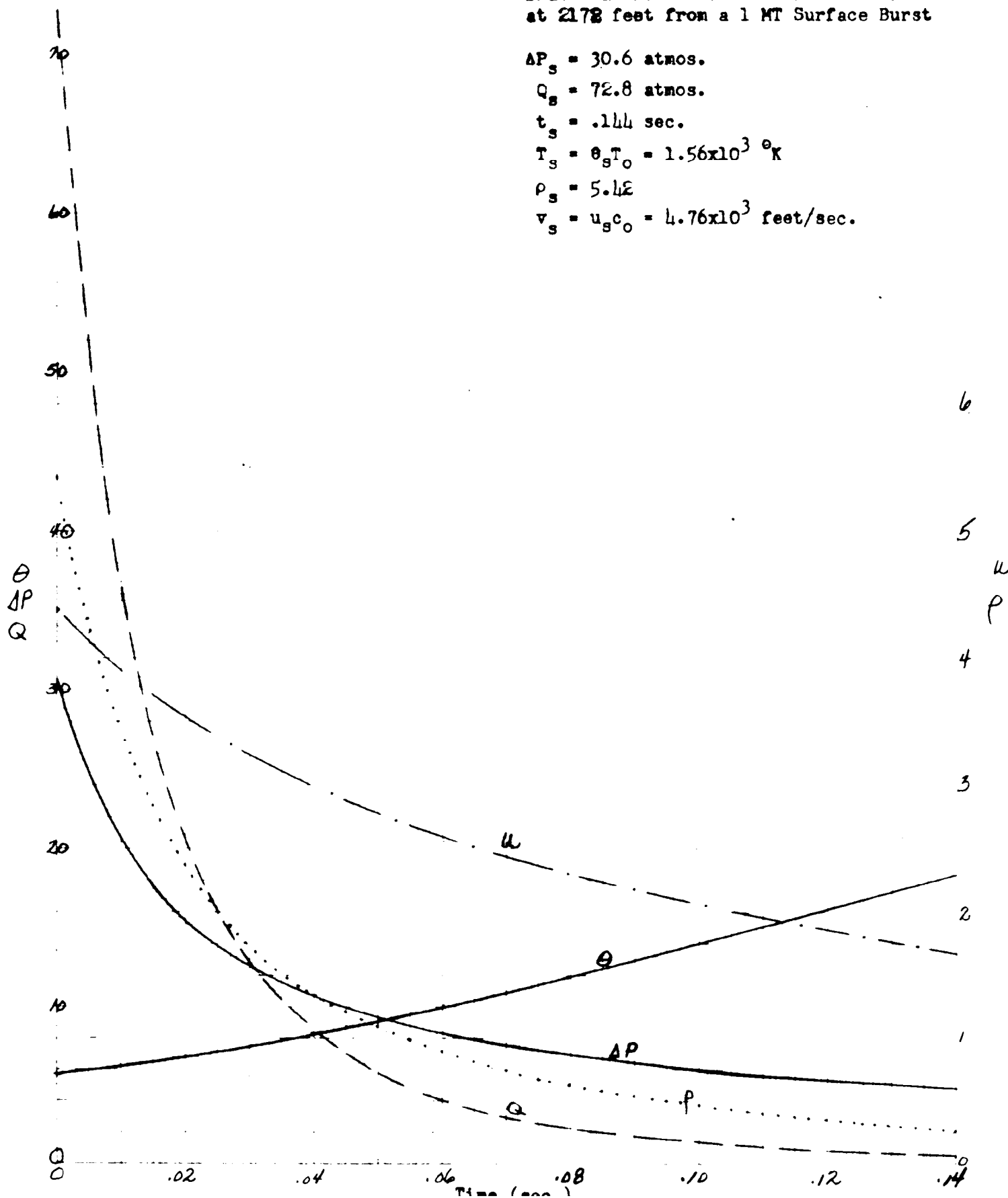


Figure 13

Blast Parameters as Functions of Time
at 2508 feet from a 1 MT Surface Burst

$\Delta P_s = 20.7$ atmos.
 $Q_s = 41.1$ atmos.
 $t_s = .205$ sec.
 $T_s = 1.19 \times 10^3 \text{ } ^\circ\text{K} = \theta_s T_o$
 $\rho_s = 4.91$
 $v_s = u_s c_o = 3.77 \times 10^3$ feet/sec.

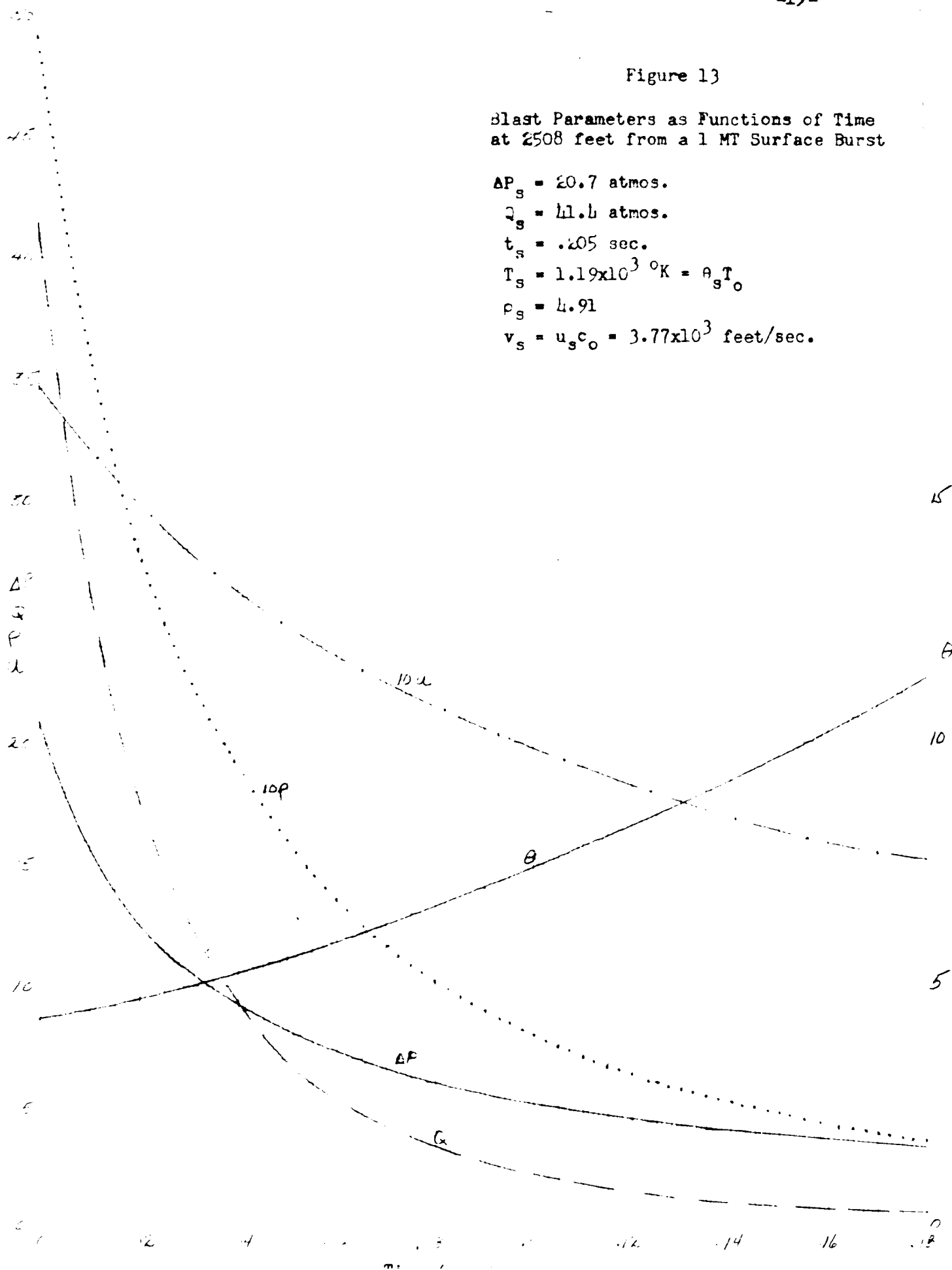


Figure 14

Blast Parameters as Functions of Time
at 2816 feet from a 1 MT Surface Burst

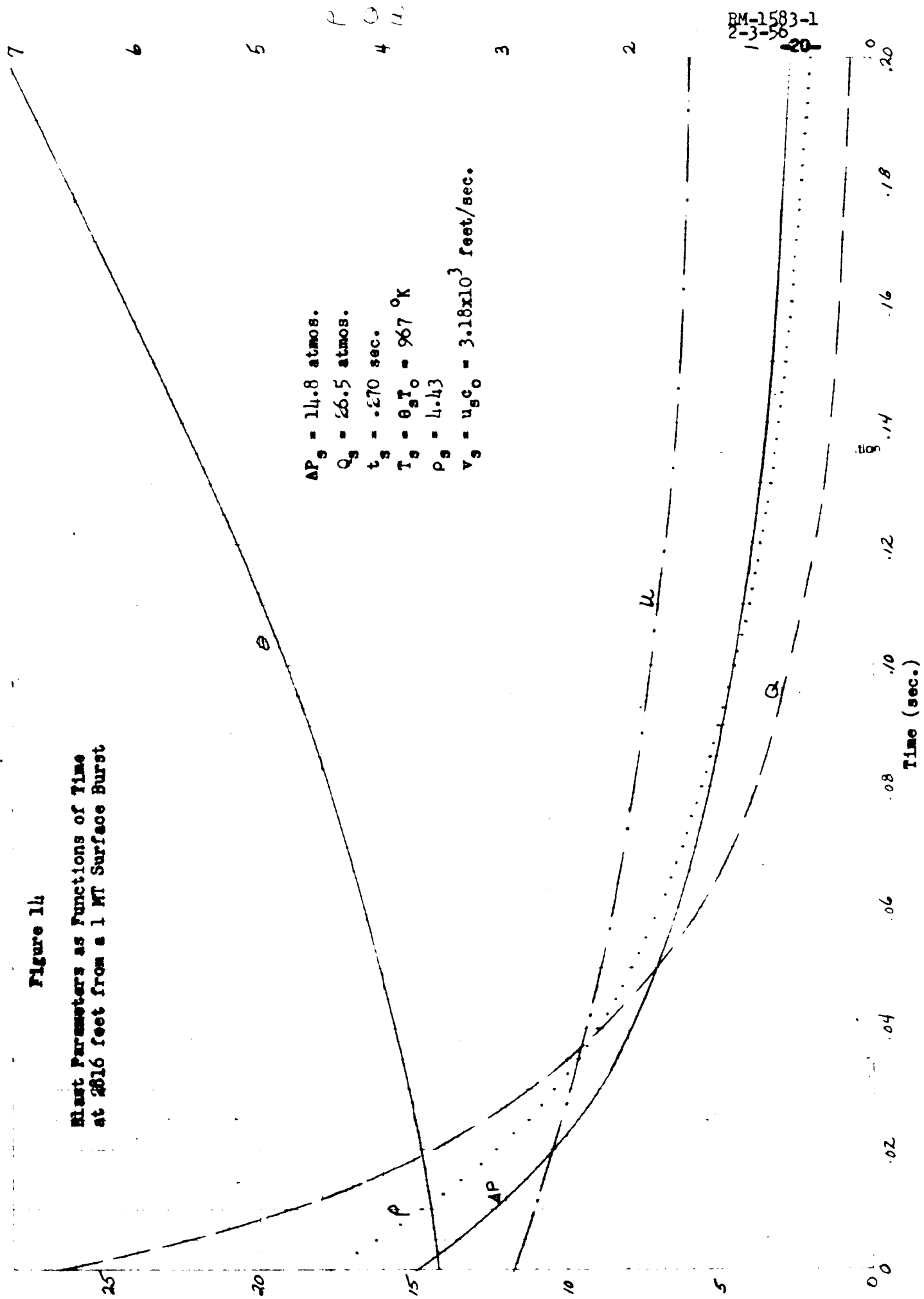
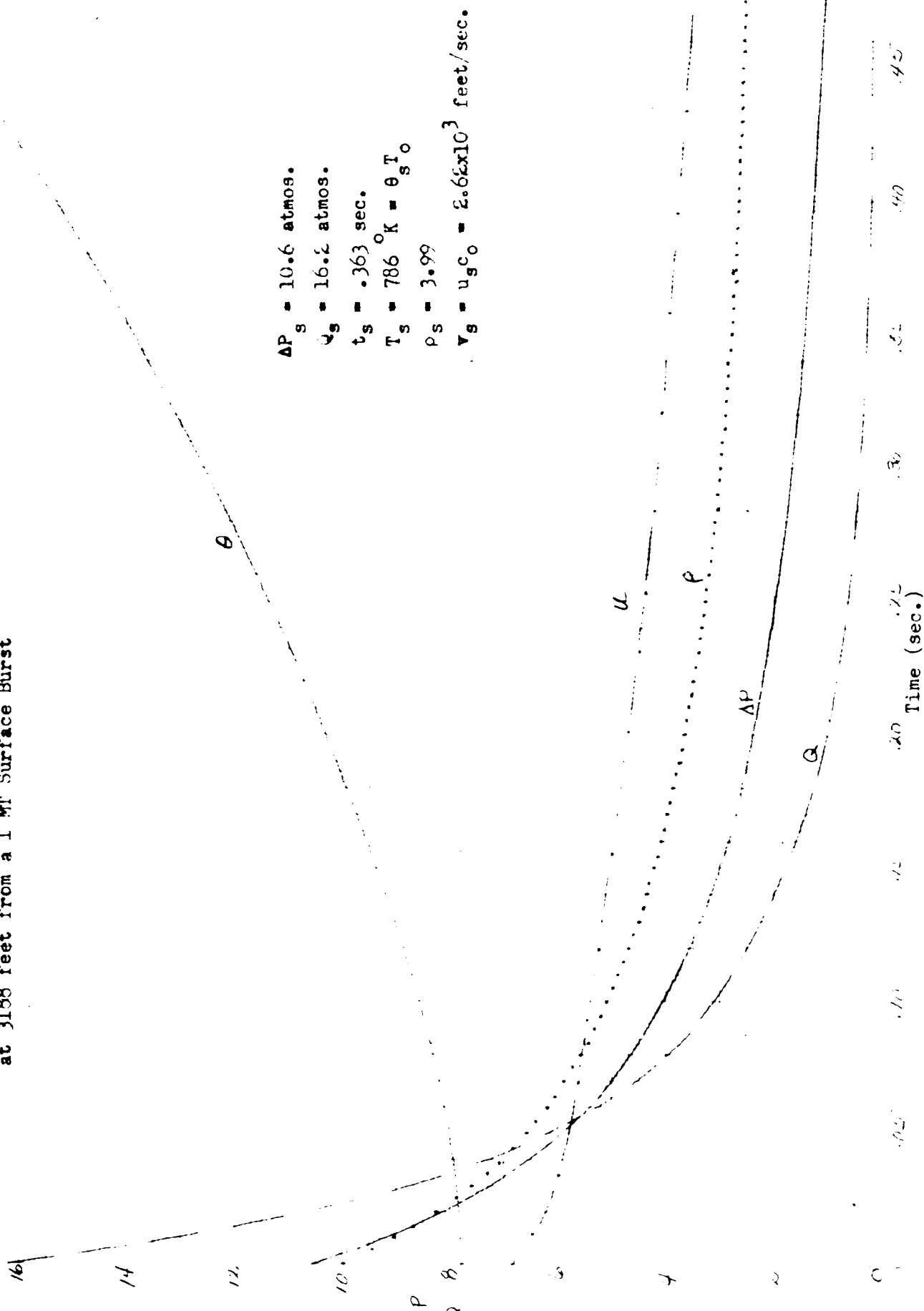


Figure 15

Blast Parameters as Functions of Time
at 3188 feet from a 1 MT Surface Burst



PM-1583-1
2-3-56
-21-

Figure 16

Blast Parameters as Functions of Time
at 3636 feet from a 1 MT Surface Burst

$\Delta P_s = 7.34$ atmos.

$Q_s = 9.46$ atmos.

$t_s = .494$ sec.

$T_s = \theta_s T_0 = 644$ °K

$\rho_s = 3.52$

$v_s = u_s c_0 = 2.13 \times 10^3$ feet/sec.

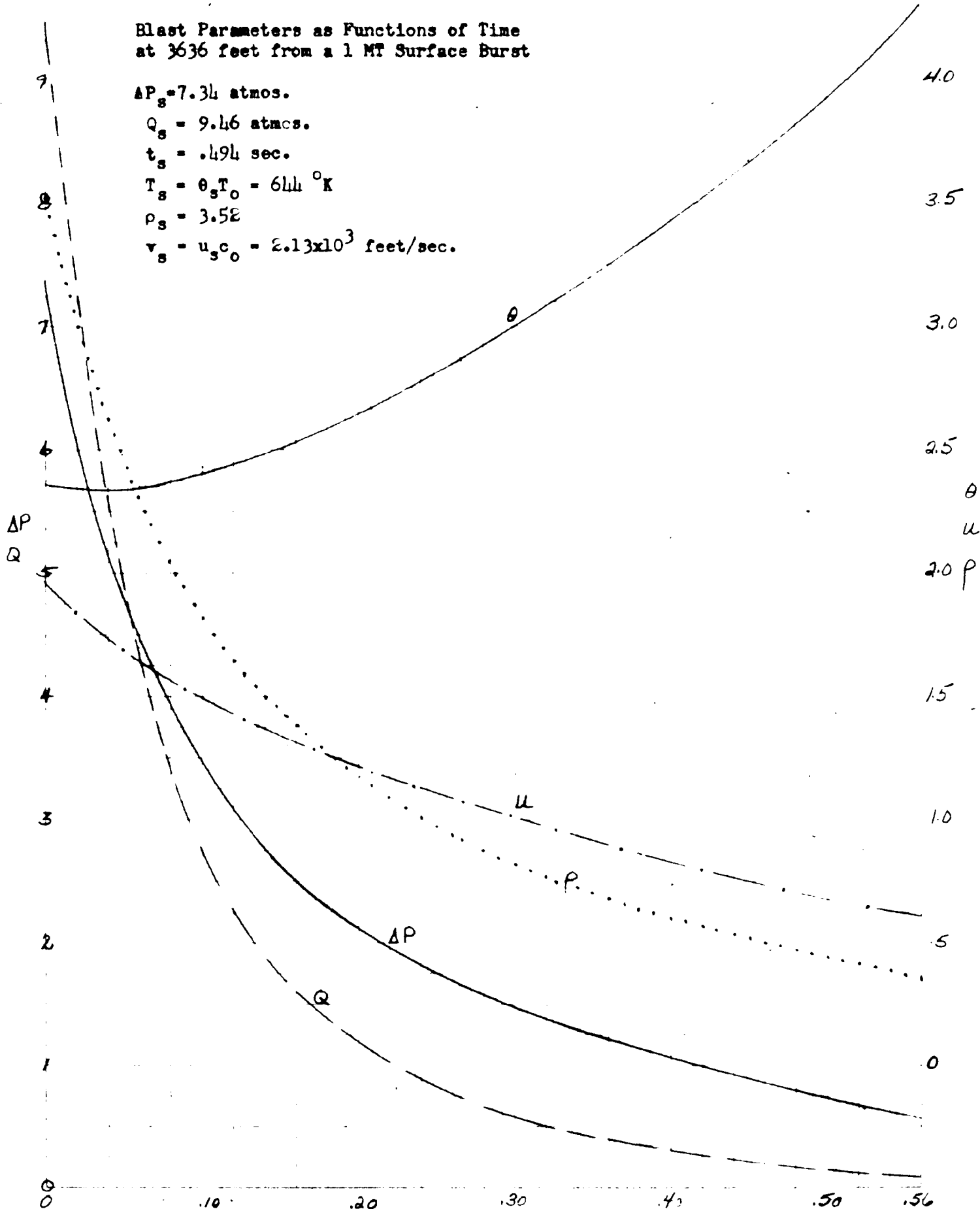


Figure 17

Blast Parameters as Functions of Time
at 4841 feet from a 1 MT Surface Burst

3.0

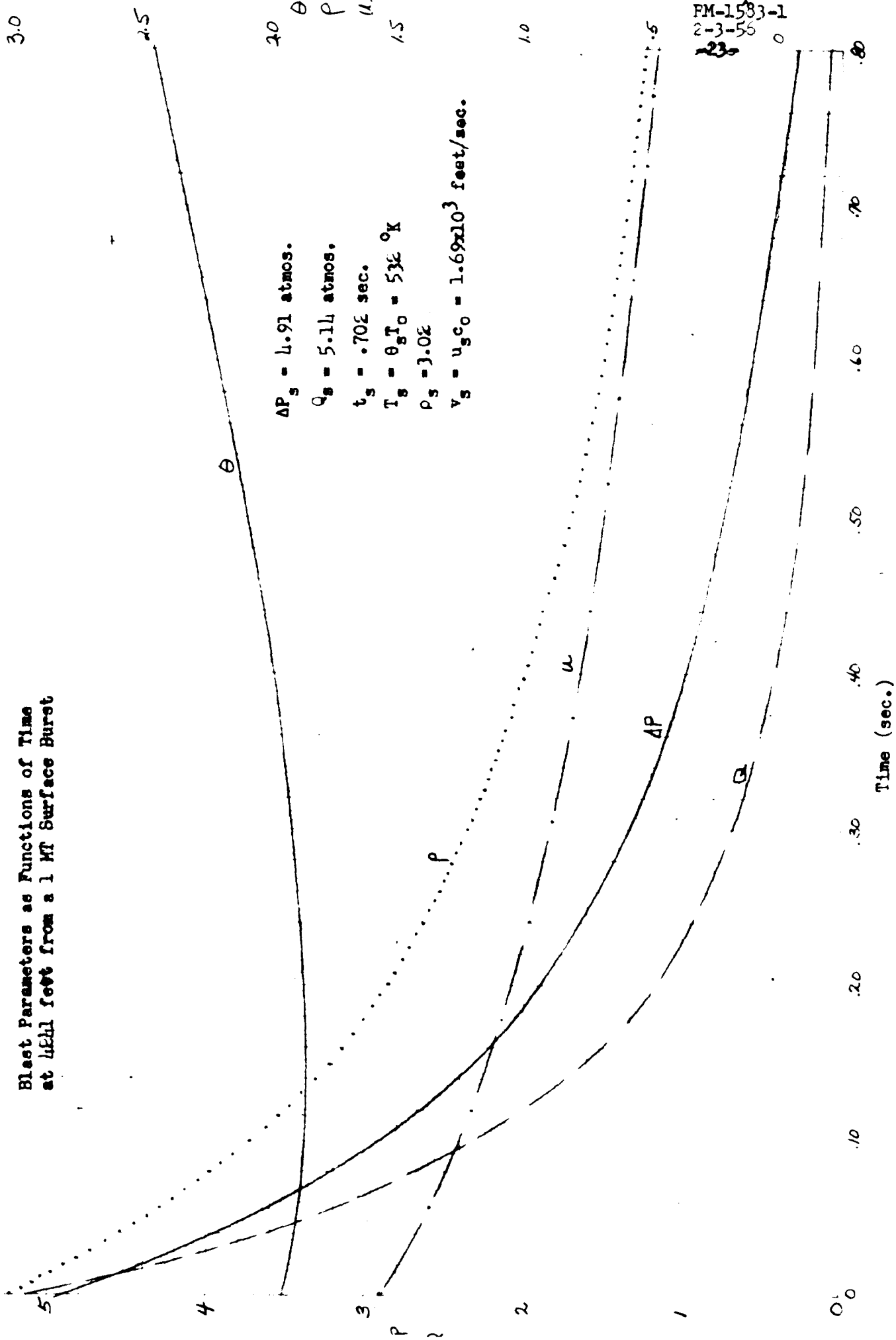
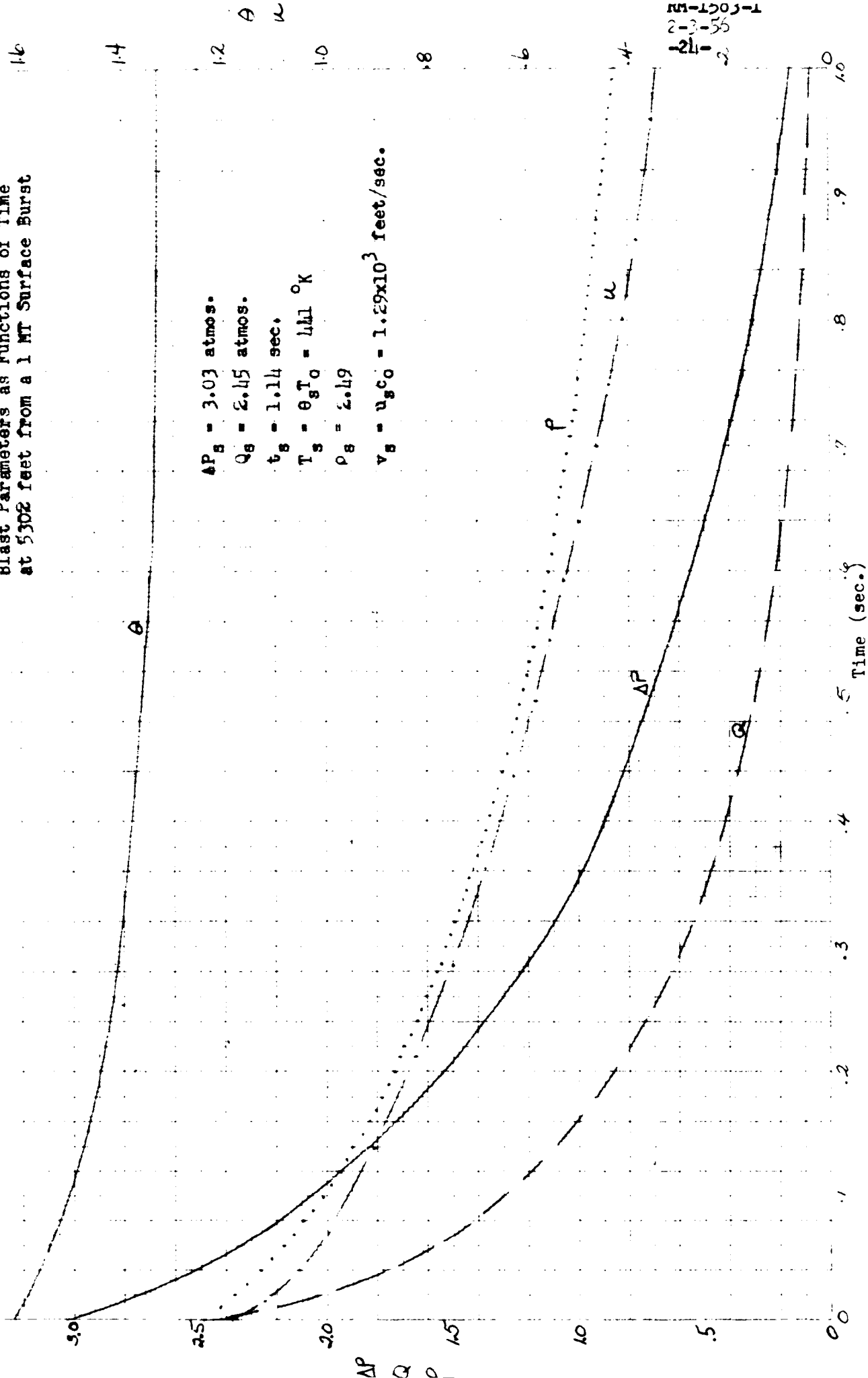


Figure 18

Blast Parameters as Functions of Time
at 5302 feet from a 1 MT Surface Burst



RM-1503-1
 2-3-56
 -21-

Figure 19

Blast Parameters as Functions of Time
at 6197 feet from a 1 MT Surface Burst

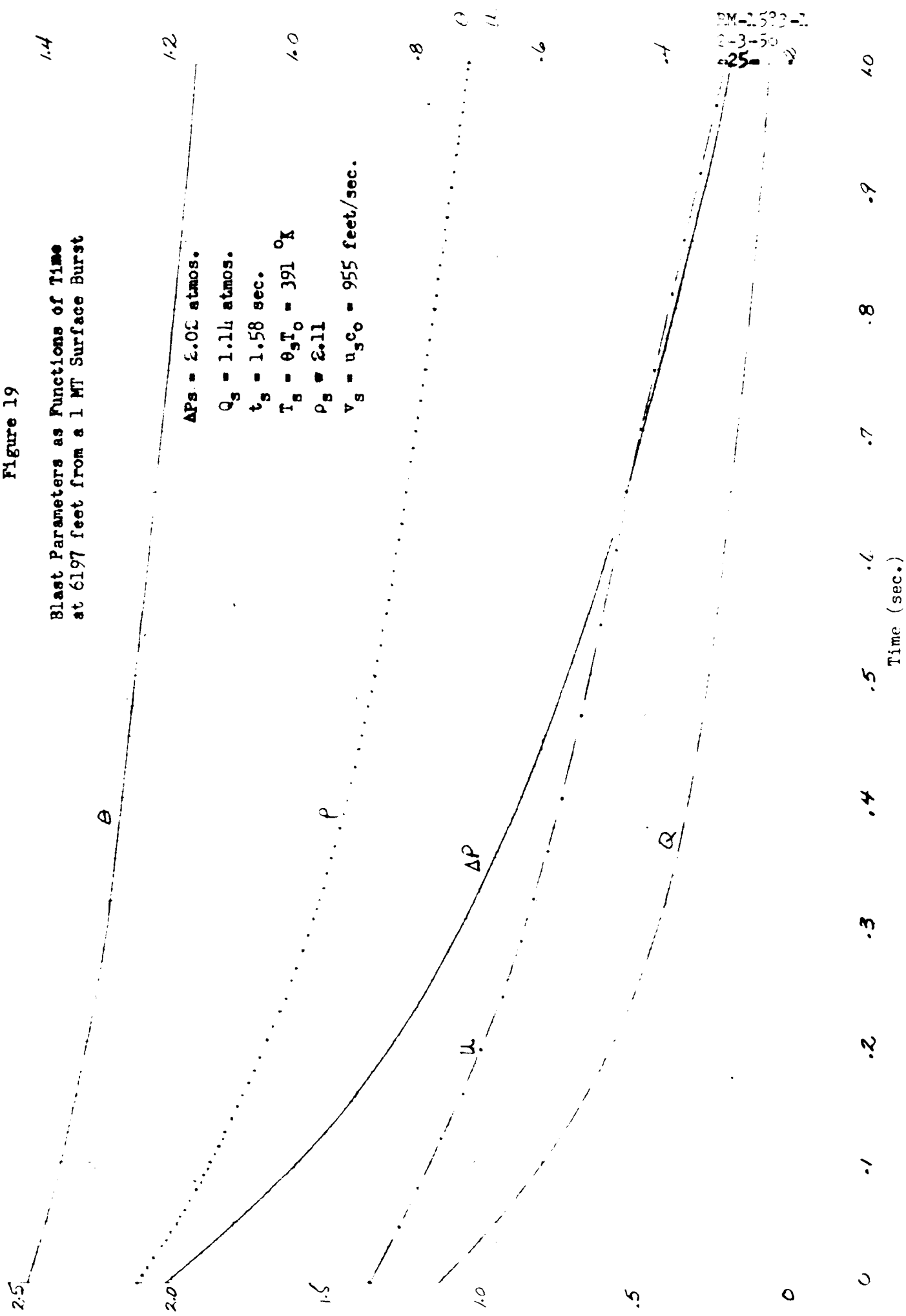


Figure 20

Blast Parameters as Functions of Time
at 8704 feet from a 1 MT Surface Burst

$\Delta P_B = .987$ atmos.
 $Q_B = .314$ atmos.
 $t_B = 3.05$ sec.
 $T_B = \theta_B T_0 = 336^\circ K$
 $\rho_B = 1.61$
 $v_B = u_B c_0 = 573$ feet/sec.

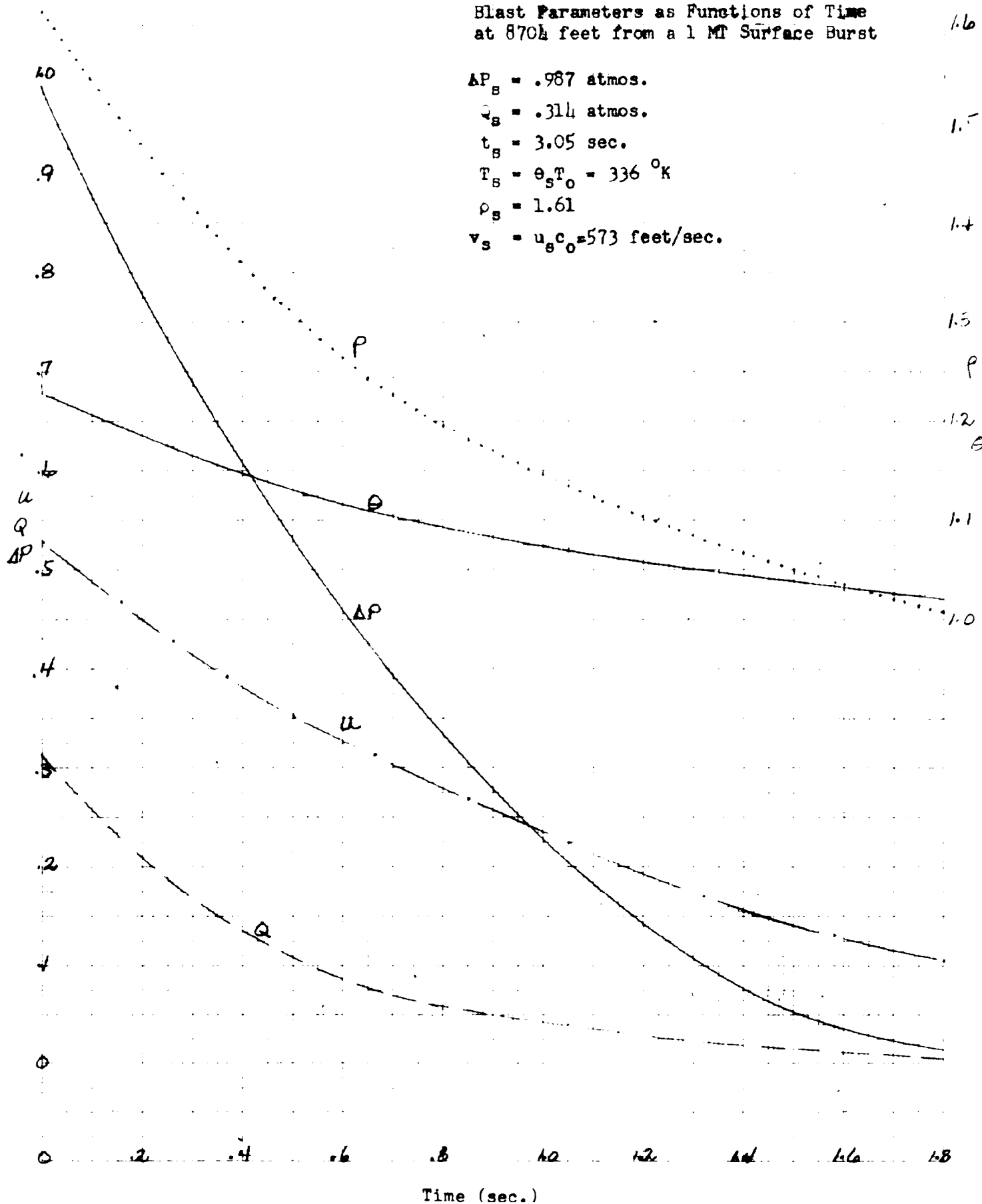
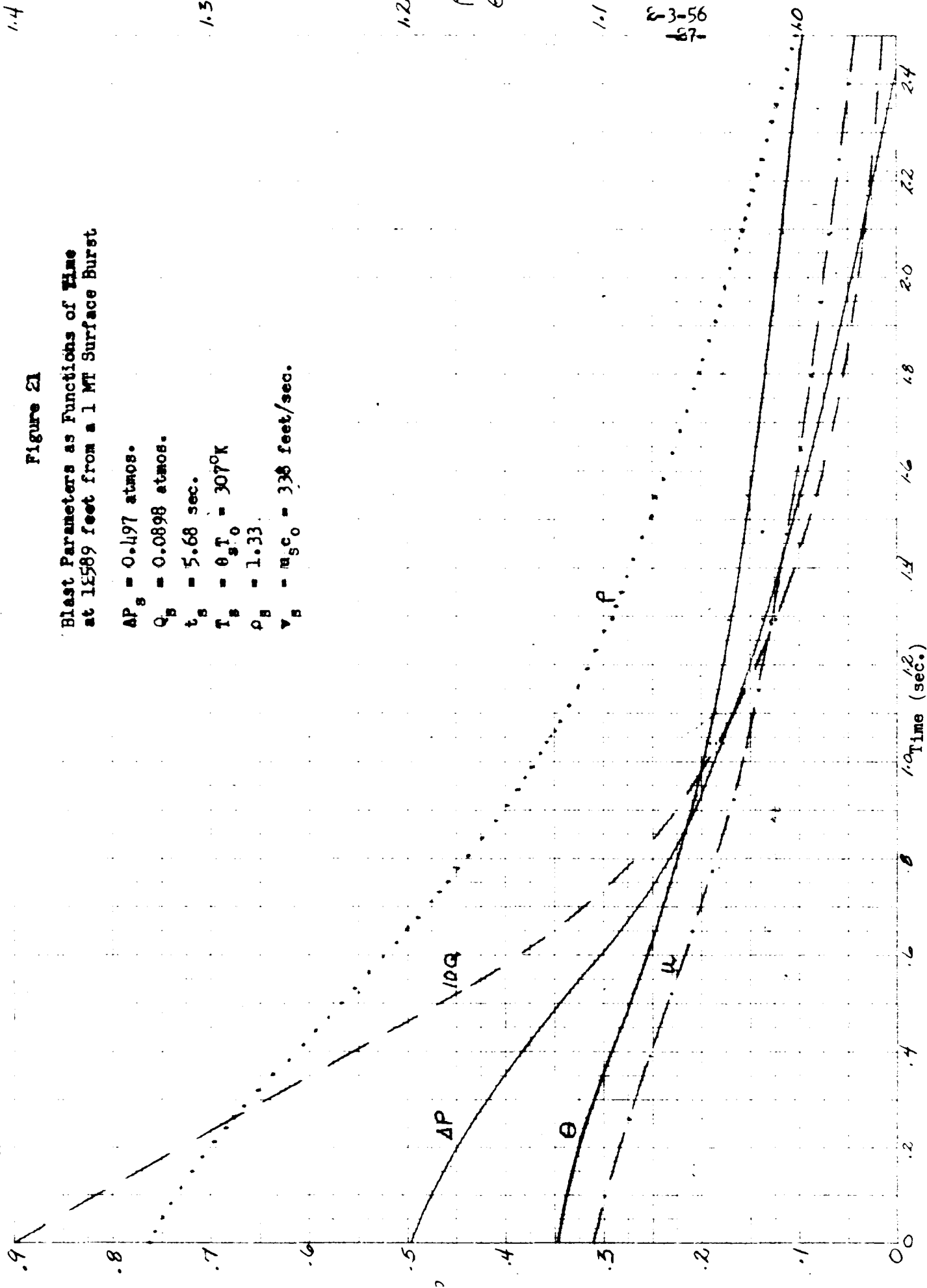


Figure 21

Blast Parameters as Functions of Time
at 14589 feet from a 1 MT Surface Burst

- $\Delta P_s = 0.497$ atmos.
- $Q_s = 0.0898$ atmos.
- $t_s = 5.68$ sec.
- $T_s = 0.7 = 307^\circ K$
- $\rho_s = 1.33$
- $v_s = u_{sc0} = 338$ feet/sec.



RM-1583-1
2-3-56
-87-

SUPPLEMENT TO RM-1583-1

CLOSE-IN H-BOMB EFFECTS

The following figures (Figure 27 and Figure 28) together with the data below represent the relations between the overpressure impulse, the dynamic impulse, the peak overpressure and the distance from a one MT surface burst. The impulses are defined as follows:

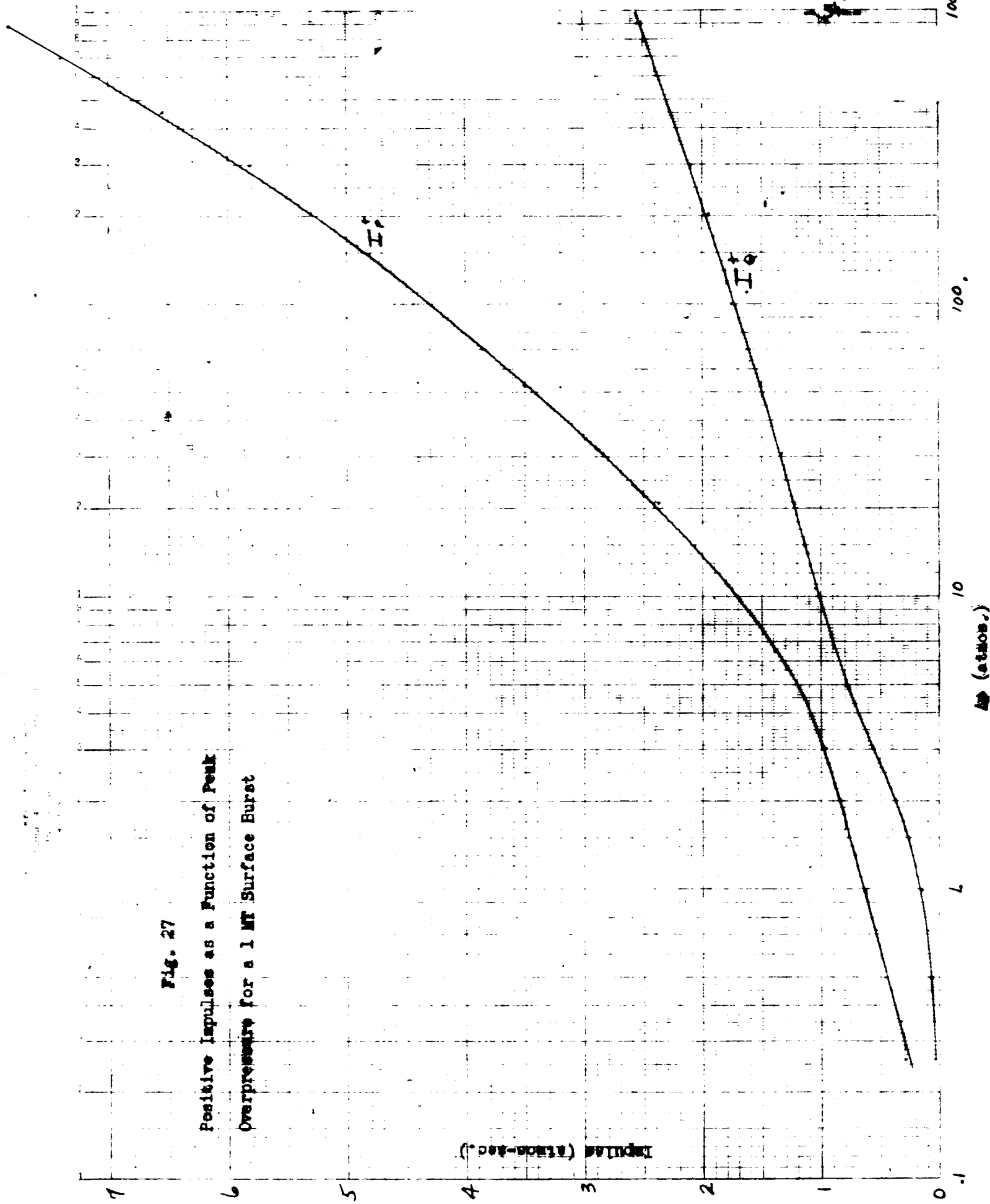
$$I_p^+ = \int_{t_s}^{D_p^+} \Delta P dt \quad (\text{atmos} - \text{sec.})$$

$$I_Q^+ = \frac{1}{2} \int_{t_s}^{D_u^+} \rho u^2 dt \quad (\text{atmos} - \text{sec.})$$

ΔP (atmos)	I_p^+	I_Q^+	R(kft)
900	7.84	2.53	.695
699	7.41	2.47	.755
452	6.55	2.27	.874
297	5.81	2.09	.994
203	5.30	1.94	1.120
99.9	4.43	1.76	1.395
69.9	3.84	1.61	1.62
52.7	3.51	1.51	1.78
30.6	2.84	1.32	2.17
20.7	2.37	1.22	2.51
14.8	2.07	1.12	2.82
10.6	1.75	1.03	3.19
7.34	1.46	0.913	3.64
4.91	1.18	0.768	4.24
3.03	0.960	0.549	5.30
2.02	0.834	0.372	6.20
0.987	0.617	0.152	8.70
0.497	0.460	0.0607	12.59

Fig. 27

Positive Impulses as a Function of Peak
Overpressure for a 1 MT Surface Burst



Positive Impulses as a Function of the
 Distance from a 1 MT Surface Burst

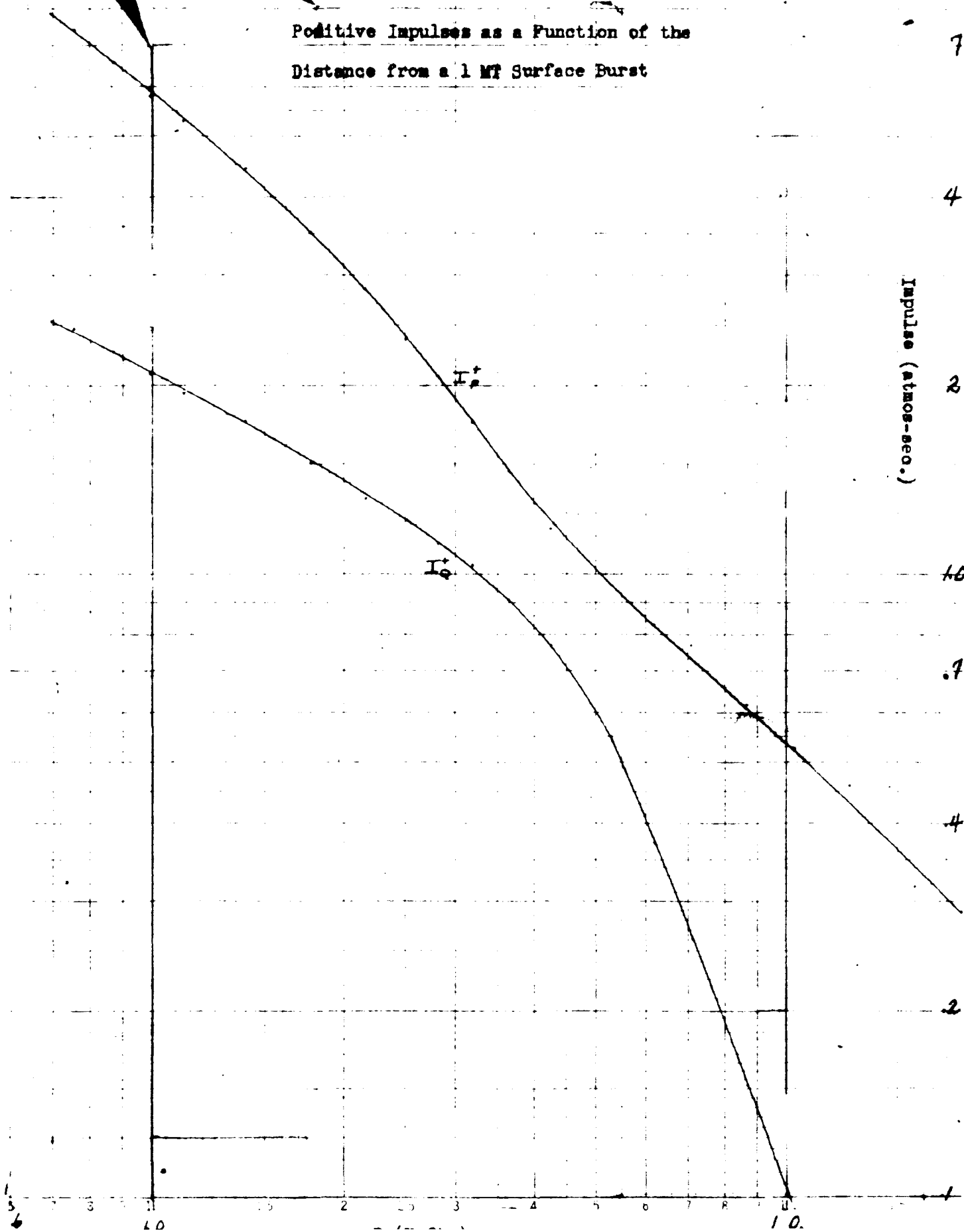
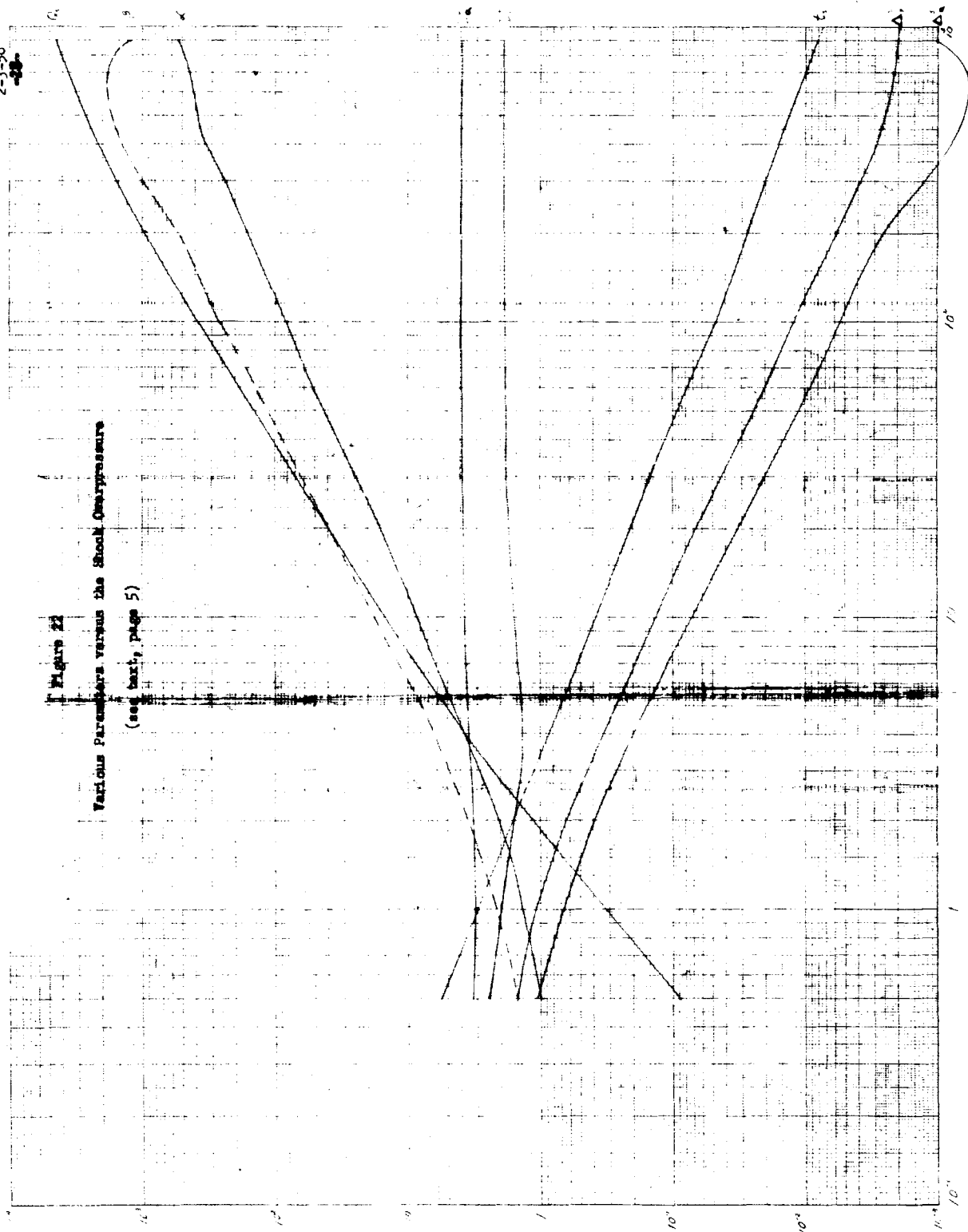


Figure 22

Various Parameters versus the Shock Overpressure
(see text, page 5)



Peak Overpressure (ΔP_0) (atmos)

Figure 23

ELAST PARAMETERS AS A FUNCTION OF RADIUS AT
 0.00807 sec. FROM A 1 MT SURFACE BURST

$$\begin{aligned}
 \Delta P_0 &= 900 \text{ atmos.} \\
 Q_0 &= 4.39 \times 10^3 \text{ atmos.} \\
 P_0 &= 8.47 \times 10^4 \text{ g./cm}^2 \\
 \theta_0 &= 50.1 = 1.37 \times 10^4 \text{ g./cm}^2 \\
 u_0 &= 27.3 = \frac{2.87 \times 10^4 \text{ feet/sec.}}{c_0}
 \end{aligned}$$

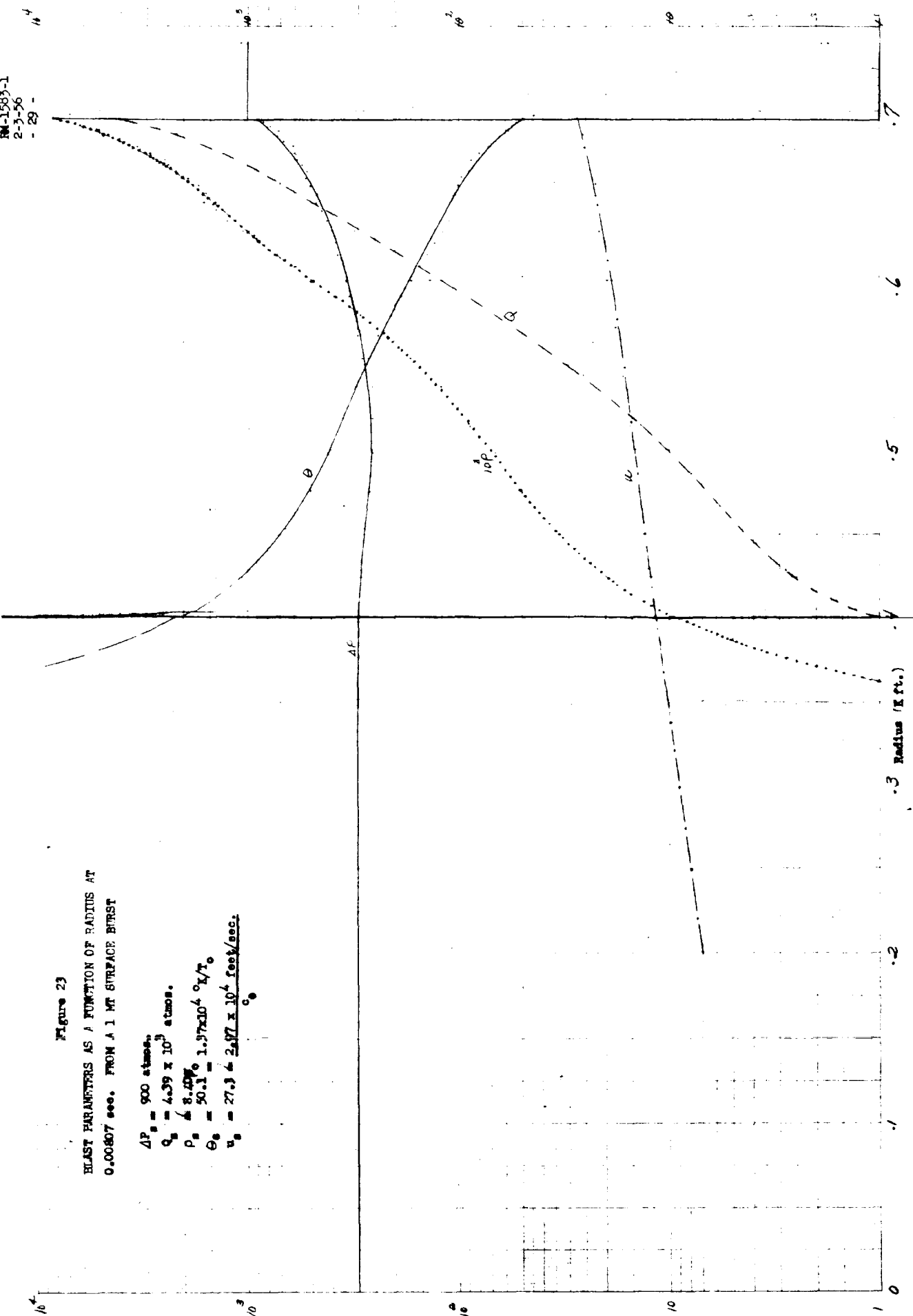


Figure 24

Blast Parameters as a Function of Radius
at 0.0699 sec. from a 1 Mt Surface Burst

$$\Delta P_s = 69.4 \text{ atmos.}$$

$$Q_s = 22\% \text{ atmos.}$$

$$P_0 = 6.86 P_0$$

$$\theta_s = 9.74 = \frac{2660^\circ K}{T_0}$$

$$u_s = 6.87 = \frac{7470 \text{ feet/sec.}}{C_0}$$

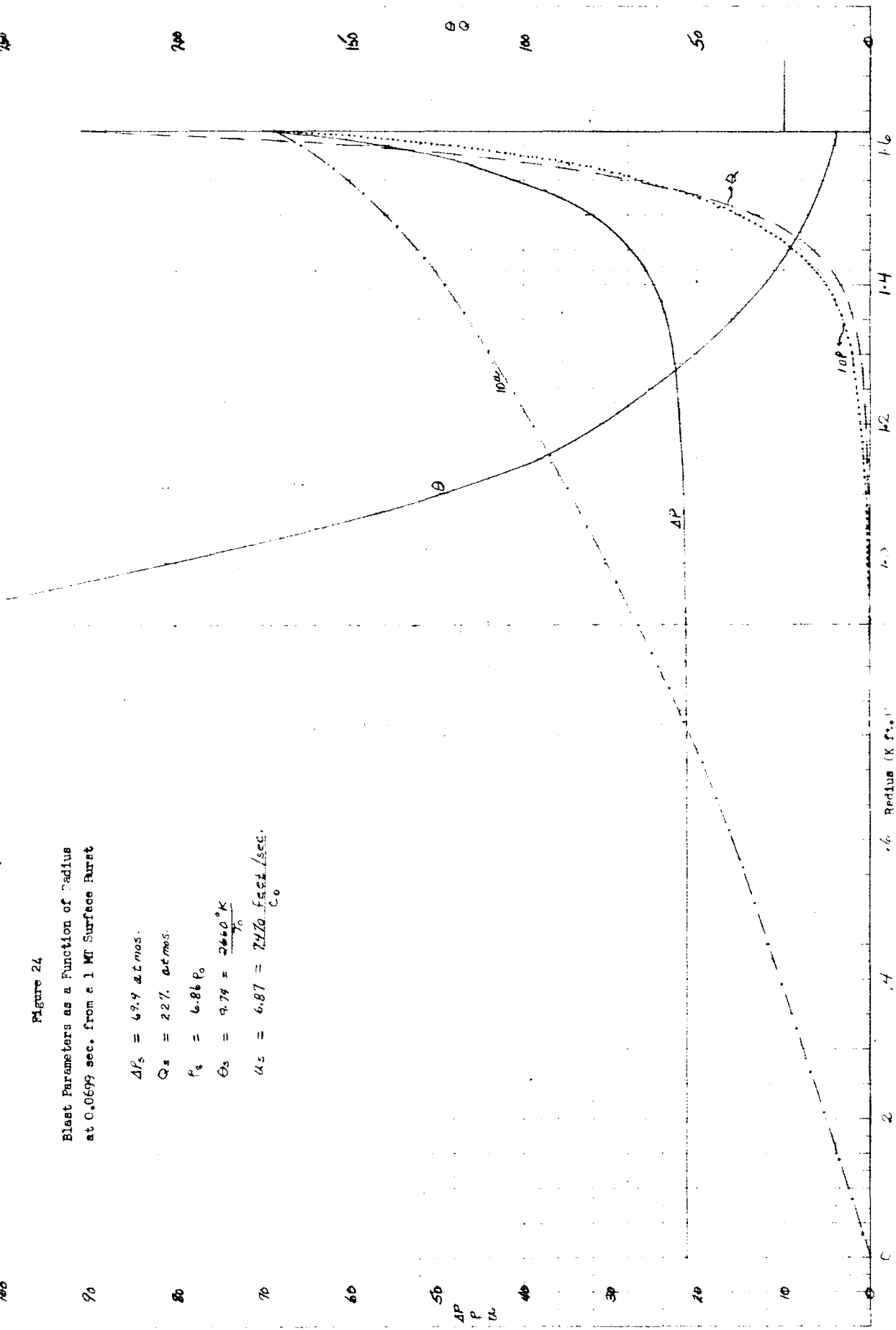


Figure 25

Blast Parameters as a Function of Radius
at 0.285 sec. from a 1 MT Surface Burst

$\Delta P_s = 20.7 \text{ atmos}$
 $Q_s = 41.4 \text{ atmos}$
 $P_b = 4.91 P_0$
 $\dot{P}_s = 4.36 = 119 \frac{\text{atm}}{\text{sec}}$
 $\dot{P}_s = 3.47 = 572 \frac{\text{feet/sec}}{r_0}$

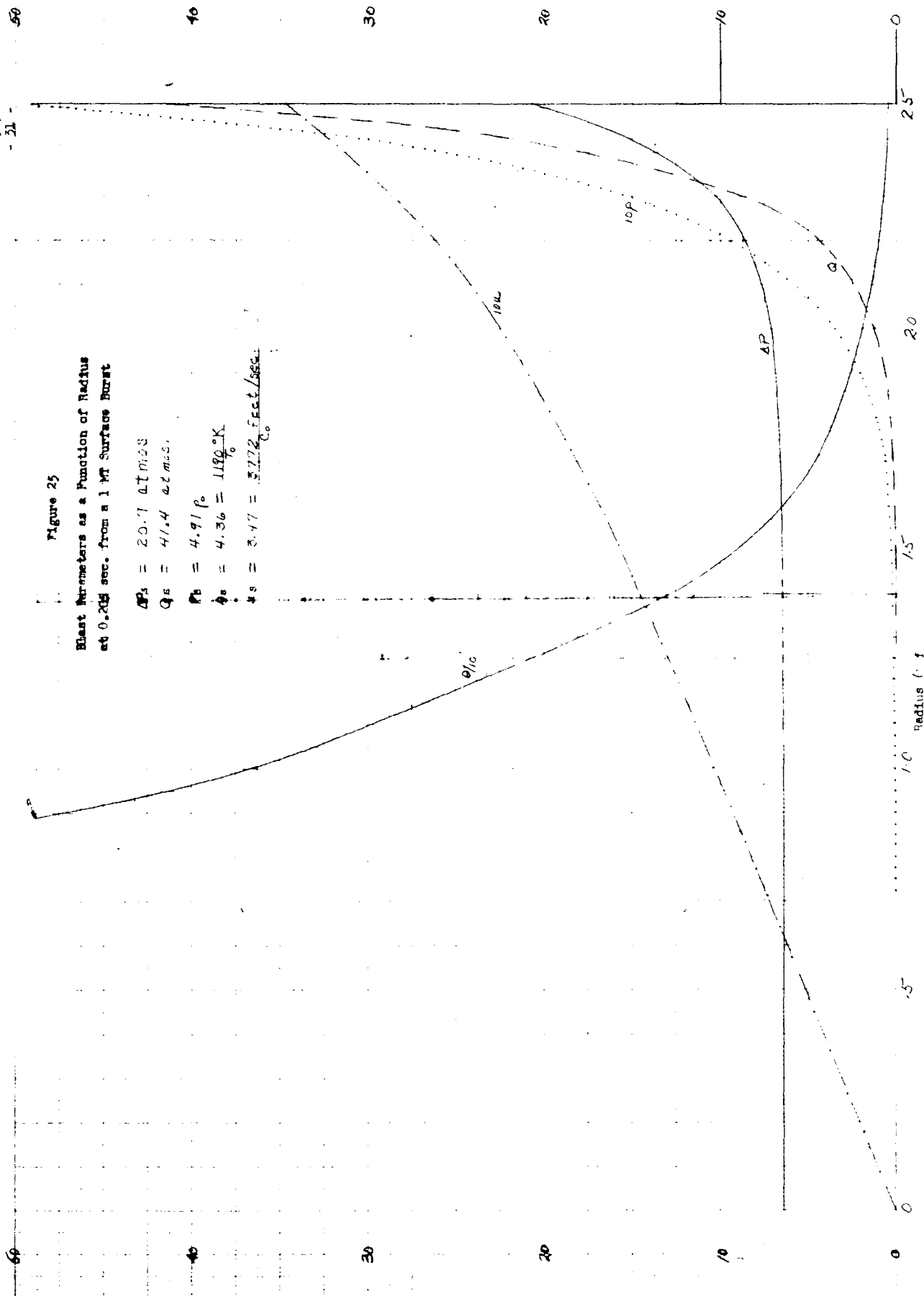


Figure B6

Elast Parameters as a Function of Radius
at 0.494 sec. from a 1 MT Surface Burst

$$\Delta P_s = 7.34 \text{ atmos}$$

$$Q_s = 9.46 \text{ atm/s.}$$

$$\rho_s = 3.52 \rho_o$$

$$\theta_s = 2.36 = \frac{6.44^\circ K}{T_o}$$

$$u_s = 1.96 = \frac{2131 \text{ feet/sec.}}{C_o}$$

